THE MODIFIED VLASOV FOUNDATION ON NONLINEAR SOIL LAYERS

A Thesis Submitted to
the Graduate School of Engineering and Sciences of
İzmir Institute of Technology
in Partial Fulfilment of the Requirements for Degree of

MASTER OF SCIENCE

in Civil Engineering

by
Mehmet ÇEREZCİ

December 2021
İZMİR

ACKNOWLEDGMENTS

I am grateful to my supervisor Assist. Prof. Dr. Volkan İŞBUĞA for giving me the chance to work with him. I am very thankful for his guidance, support, encouragement, and patience throughout my thesis.

I would also like to thank my thesis committee members Prof. Dr. Mehmet Zülfü AŞIK and Prof. Dr. Nurhan ECEMİŞ ZEREN for their valuable insight and suggestions.

I am very grateful to my parents, Şerife and Hasan ÇEREZCİ and my sister, Safiye ÇEREZCİ for their support and love.

I would also like to thank Miray BÜYÜK for her understanding, encouragement, endless patience and love.

Lastly, I am thankful for all my friends for their friendship, endless support, and encouragement.

ABSTRACT

THE MODIFIED VLASOV FOUNDATION ON NONLINEAR SOIL LAYERS

In this thesis, a novel approach to account for the soil nonlinearity of nonhomogeneous soil deposits by employing the modified Vlasov foundation model is developed. A new algorithm that takes the modulus degradation curves at varying strain levels into account in an iterative manner is obtained by modifying the previously developed formulation. The presented model will provide researchers with the opportunity to employ the experimental test data directly for an operational strain level that may occur in many foundation engineering designs. This new model which takes the nonlinear soil behavior into account is first verified against the linear model given in the literature to ensure that the new model algorithm can capture the linear solution when the soil behavior is assumed to be linear. Later, the experimental data of modulus reduction curves reported in the literature for a specific type of dense and loose sands are used in multiple foundation deflection analyses. Example problems are considered for different cases which presented: (i) how the model captures nonlinear behavior and (ii) the significant effect of the nonlinear soil behavior on deflection, moment, and shear force. The model results are also compared with the finite element model result, assuming a bilinear stress-strain soil model. The results obtained from both models matched well, especially for the maximum deflection values that occurred in the example problems.

ÖZET

DOĞRUSAL OLMAYAN ZEMİN ÜZERİNDEKİ DEĞİŞTİRİLMİŞ VLASOV TEMELİ

Bu tezde, modifiye edilmiş Vlasov temel modeli kullanılarak homojen olmayan zeminlerin doğrusal olmayan davranışını hesaba katan yeni bir yaklaşım geliştirilmiştir. Bu yeni algoritma, değişen gerinim seviyelerindeki modül azaltma eğrilerini yinelemeli olarak hesaba katacak şekilde var olan formülasyon geliştirilerek elde edilmiştir. Sunulan model araştırmacılara temel mühendislik tasarımlarında oluşabilecek işlevsel gerinim seviyelerinde, deneysel test datalarını direkt kullanma imkânı sağlamaktadır. Doğrusal olmayan zemin davranışını hesaba katan bu yeni model, doğrusal çözümü yakalayabildiğini göstermek için ilk olarak literatürde verilen doğrusal modele karşı doğrulanmıştır. Daha sonra, literatürde verilen modül azaltma eğrilerinin verileri kullanılarak belirli bir çeşit sıkı ve gevşek kum için çeşitli temel deplasman analizleri gerçekleştirilmiştir. Farklı durumlar için örnek problemler: (i) modelin nasıl doğrusal olmayan davranışı yakaladığı ve (ii) doğrusal olmayan zemin davranışının deplasman, moment ve kesme kuvveti üzerindeki belirgin etkisi. Modelin sonuçları aynı zamanda sonlu eleman modeli sonuçları ile bi-lineer gerilme-gerinme zemin modeli varsayılarak karşılaştırılmıştır. Her iki modelin sonucunda elde edilen sonuçlar özellikle meydana gelen maksimum deplasman değerleri için birbirleriyle iyi eşleşme göstermiştir.

TABLE OF CONTENTS

LIST OF FIGURES

Figure **Page**

Figure **Page**

CHAPTER 1

INTRODUCTION

Modeling the behavior of foundations considering the soil-structure interaction accurately under vertical loads has attracted the interest of researchers for years because foundations are important structural components that transfer the loads from the superstructure to the underlying soil layers. There are many soil-structure interaction models in the literature and these models have been used and developed by researchers over time for different foundation types and soil layering some of which are explained in Chapter 2 Literature Review. Using different assumptions and physical models, researchers obtained the differential equations for those foundation-soil systems. Besides, various software packages employing the theory of the finite element are used to analyze engineering problems in this field; but they contain various limitations, for instance, (i) expertise on software which is required for the effective use of such commercial software packages, (ii) limitations on the implementation of new approaches and methods, and (iii) expensive license prices and maintenance. Therefore, researchers continue to produce and develop models with new methods on this subject.

In this study, we propose a new model and algorithm to account for soil nonlinearity in the form of modulus reduction curves. Although there exist advanced soil models already implemented and used in association with various software packages as aforementioned above, the aim of this study is to develop a practical analysis method that employs the well-known soil mechanics test results without multiple parameter determination tests for advanced soil constitutive models. In this context, the modulus reduction curves which are often used in the dynamics analyses of soil layers for example site response analysis were employed in this study. It has been also shown in the literature that modulus reduction curves obtained by monotonic loadings can be also applied to problems in which loads are increased incrementally as we follow in this study.

Unlike the similar methods proposed for foundation-soil interaction modeling in the literature, this study proposes a method that accounts for shear modulus reduction curves versus shear strain occurring in the soil and/or Young's (Elasticity) modulus reduction curves versus axial strain, both of which can be determined by standard soil mechanics

experiments. In this scope, we developed a new approach and extended a previously developed foundation-soil interaction model that assumes soils as a linear elastic material to account for soil nonlinearity so that we include more realistic soil behavior in a practical manner. Thus, an approach that includes realistic soil behavior will be incorporated into a soil-structure interaction model that considers the continuous nature of soils.

The thesis consists of six chapters. The first chapter is the introduction, the second chapter is the literature review of the existing models, the third chapter presents the numerical methodology developed in this study, and the fourth chapter presents the numerical examples including comparisons with some existing methods. Lastly, the fifth chapter, the final chapter, presents a discussion of the results.

CHAPTER 2

LITERATURE REVIEW

2.1. Soil Structure Interaction Models

Soil-structure interaction analysis is generally divided into two categories. The first one is the direct method and the second one is the sub-structuring method (Kramer, 1996). Many researchers have investigated the effect of the soil-structure interaction on the structural response using these general methods of analysis. In the sub-structure method, the soil and structure are divided in separate parts. These models consider simplified linear or nonlinear behavior for soil. The direct method assumes both the soil and structure as a system. It is defined as the “complete solution” by Seed et al. (1977). It is the most common approach to involve nonlinear numerical analysis of a detailed model of the structure which is constructed from the three-dimensional geometry of the structure (Seed et al., 1977). But in this work, we only focus on the foundation-soil interaction model, and we can classify them as discrete models and continuous models which are part of the direct approach. The classification of soil-structure interaction models are shown in Figure 2.1.

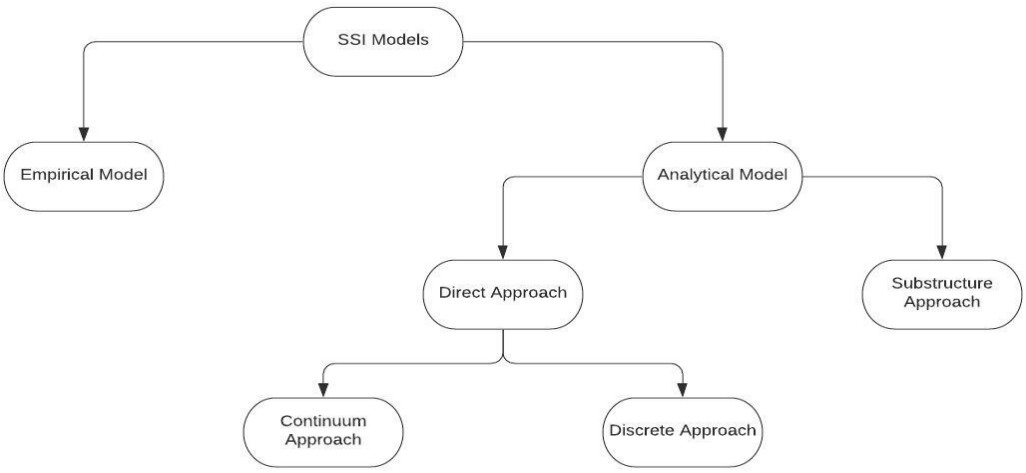

Figure 2.1. Classification of soil-structure interaction models

(modified from Zadeh, 2020)

2.1.1. Discrete Approach

The discrete approach is the simplest method to represent the effect of soil by sets of individual springs which are attached to the foundation. Also, dashpots and a shear layer can be combined with springs to improve the model. The properties of these discrete elements depend on the characterization of soil. This approach cannot be applied to all aspects of soil-structure interaction. For instance, as is, it is insufficient for calculating kinematic effects and simulation of dynamic pore water pressure in the soil.

Because of its simplicity, many researchers have used this approach for the modeling of soil-structure interaction. In this section, we introduce some of the well-known models of the pioneers in the field such as Winkler (1867), Filonenko-Borodich (1940, 1945) and Pasternak (1954). Dutta and Roy (2002) and Braja M. Das (2010) reviewed the existing models in the literature. Some of the models explained by Dutta and Roy (2002) and Braja M. Das (2010) are summarized below.

2.1.1.1. The Winkler Model

One of the most well-known methods in the field of soil-structure interaction modeling is the beam-on-elastic soil approach proposed by Winkler (1867). Figure 2.2 shows the Winkler model, and the deflection of the foundation in the direction of the load is indicated by w in the figure. In this model, the foundation is modeled as a beam on the soil, and the soil is modeled as a system of linear springs spaced at short intervals along the beam. The springs are independent of each other but generally have the same constant. This model has been used in many studies, such as applications of dynamic problems involving soil-structure interaction. Studies in which the behavior of soils can be obtained more realistically by using nonlinear springs have also been added to the literature (Kagawa and Kraft 1980; Badoni and Makris 1996; Boulanger et al., 1999; El Naggar

and Bentley, 2000; Rha et al., 2004; Gerolymos and Gazetas, 2005; Allotey and El Naggar, 2008, Younesian et al., 2019).

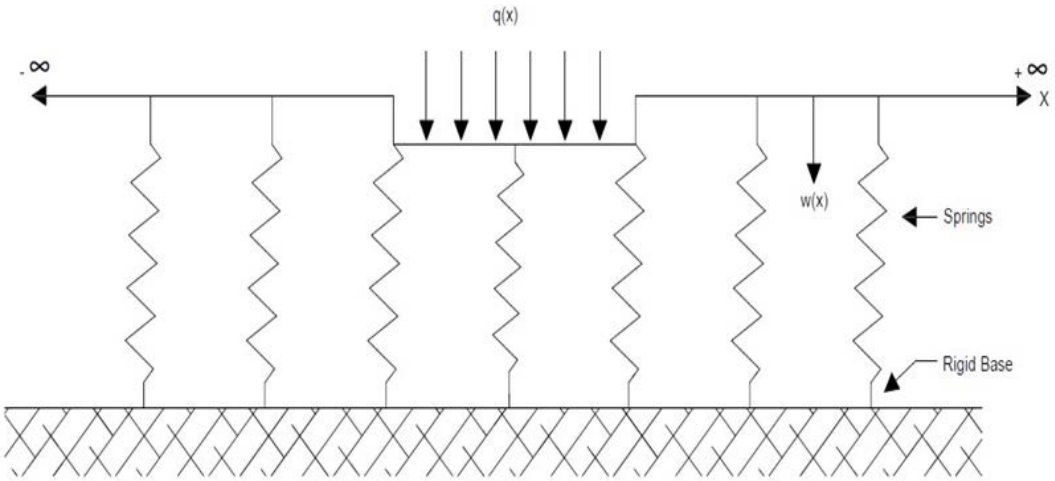

Figure 2.2. Winkler model

(modified from Braja M.Das, 2010)

In the Winkler model shown in Figure 2.2, the soil strength parameters are associated with the spring constants *k*, but these constants cannot be obtained directly from soil mechanics laboratory tests. For this reason, there are also studies to find the spring constants representing the soil strength and to find the relationships between the shear strength parameters of the soil (Chandra et al., 1987; Daloglu and Vallabhan, 2000; Dutta and Roy, 2002; Bhartiya et al., 2020).

2.1.1.2. The Filenenko-Borodich Model

Unlike the Winkler model, the Filonenko-Borodich model takes the interaction between each spring element into account. The connection of these springs elements is provided

with thin elastic membranes under a constant tension *T* (Kerr, 1964). Figure 2.3 below shows this model.

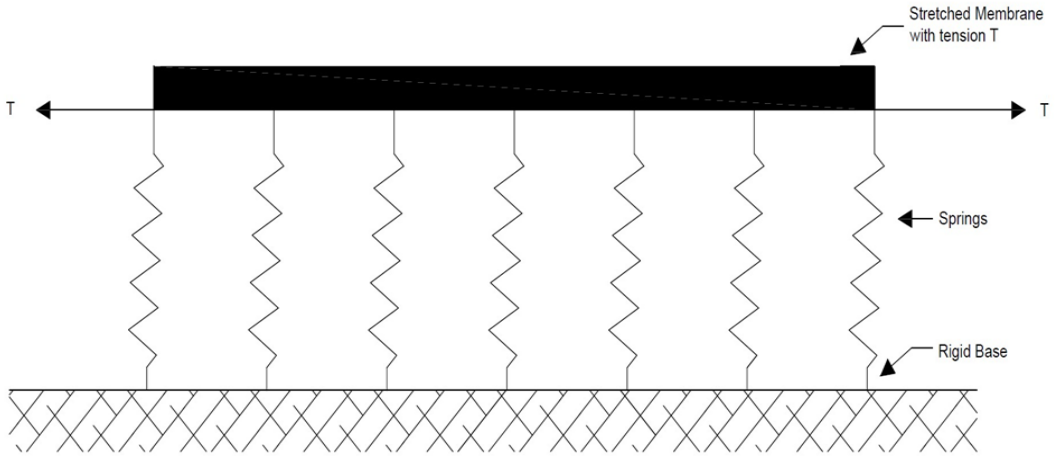

Figure 2.3. Representation of Filonenko-Borodich model

(modified from Kerr, 1964)

The pressure-deflection equation of the model can be expressed as follows.

$$p(x,z) = kw(x,z) - T\nabla^2 w(x,z) \tag{2.1}$$

$$\nabla^2 = \frac{\partial^2}{\partial x^2} + \frac{\partial^2}{\partial z^2} \tag{2.2}$$

where *p* is applied pressure, *w* is deflection of the soil and it is continued in the same manner for other models following below, ∇^2 is Laplace operator, and *T* is tensile force.

2.1.1.3. The Pasternak Model

The Pasternak model is an improved approach of the Winkler model by using two foundation parameters which are the subgrade reaction modulus and the Pasternak parameter (Kerr, 1964). This model considers the shear interaction between separate

spring elements (Wang et al. 2001; Chen et al. 2004). This model can be demonstrated in Figure 2.4.

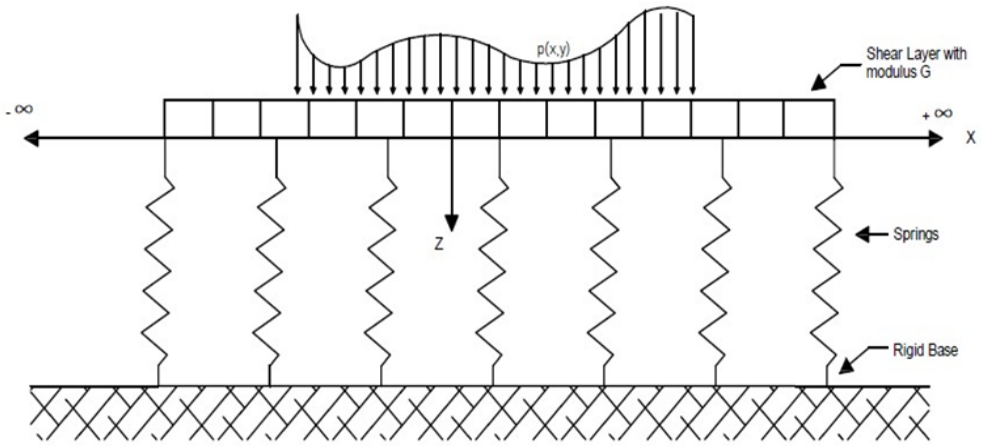

Figure 2.4. Representation of Pasternak foundation

(modified from Braja M.Das, 2010)

This model expresses the beam or plate deforming only in transverse shear. The force equilibrium of the shear layer in the z-direction yields the load-deflection relationship. The pressure-deflection equation is expressed as follows.

$$p(x,z) = kw(x,z) - G\nabla^2 w(x,z) \tag{2.3}$$

where G is the shear modulus of the shear layer. The difference between of this model and Filonenko-Borodich model is that the constant tension T is used instead of G.

2.1.1.4. The Kerr Model

In this model, a shear layer that has the different spring constants above and below the layer is introduced in the model formulation. The physical depiction of this model is shown in Figure 2.5. (Kerr, 1965). The governing differential equation for the model can be given as follows.

$$\left(1+\frac{k_2}{k_1}\right)p = \frac{G}{k_1}\nabla^2 p + k_2 w - G\nabla^2 w \tag{2.4}$$

where k_1 is the first layer's spring constant, k_2 is the second layer's spring constant, and w is the first layer's deflection.

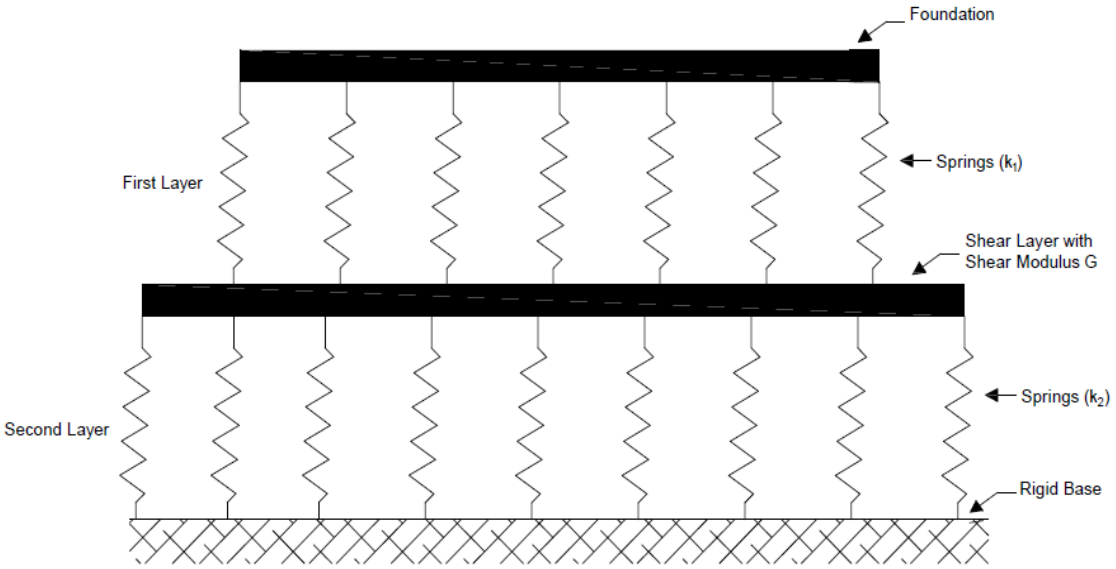

Figure 2.5. Representation of Kerr model

(modified from Dutta and Roy, 2002)

2.1.1.5. The Hetenyi Model

The Hetenyi model considers that the reaction of springs is also not independent. The link between the Winkler model springs is provided by an Euler–Bernoulli beam or a thin plate for one-dimensional problems and two-dimensional problems, respectively (Younesian et al., 2019). Figure 2.6 depicts a beam or plate with a solely bending reaction and no mass. The following equation expresses the relationship between force and displacement through this foundation.

$$p(x,z) = kw(x,z) + k_1 \frac{\partial^2 w(x,z)}{\partial x^2} \tag{2.5}$$

where $k_1 = EI$ being the flexural rigidity of the beam, or $k_1 = D$ being flexural rigidity of the plate.

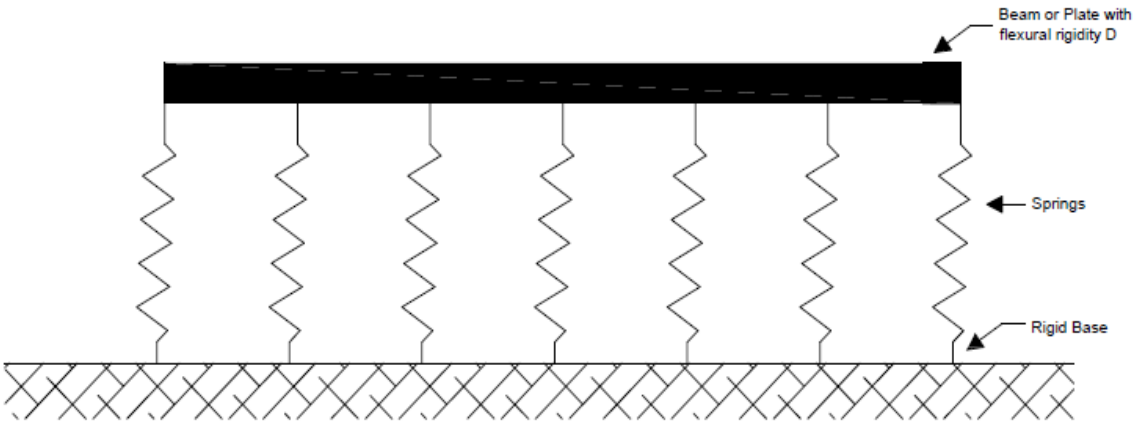

Figure 2.6. Representation of Hetenyi model

(modified from Dutta and Roy, 2002)

2.1.1.6. The New Continuous Winkler Model

In order to simulate the soil continuity, additional structural elements are incorporated. This model does not use separate discrete Winkler springs but intermeshed Winkler springs instead to allow for connectivity (Dutta and Roy, 2002). In Figure 2.7, some springs that are not directly attached to the foundation, are providing interconnection among Winkler springs which are connected to the beam or plate representing the foundation at one end and the rigid base at the other end. This contribution of the model resides in its capability to consider the effect of the soil beyond the foundation's boundaries.

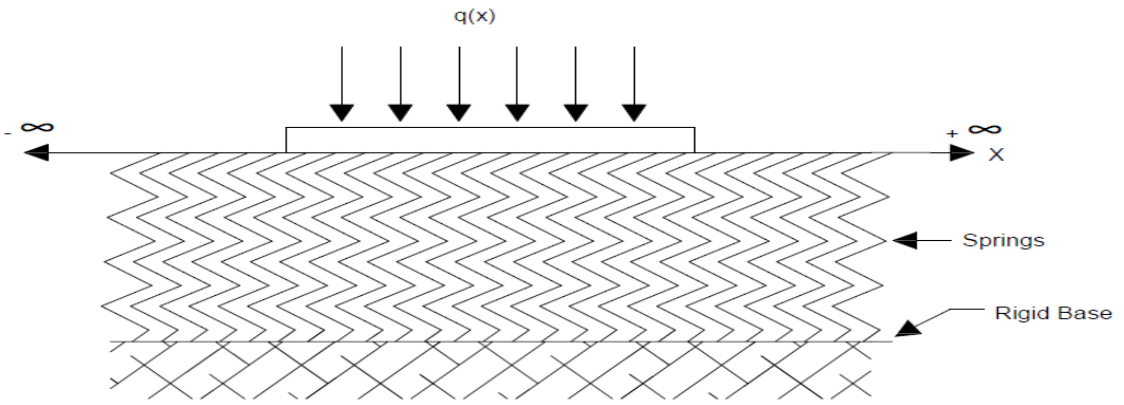

Figure 2.7. Representation of New Continuous Winkler model

(modified from Dutta and Roy, 2002)

2.1.2. Continuum Approach

The continuum approach considers the soil as a continuous medium that can capture the deformation of the soil underneath the foundation better. It proposes a rational illustration of soil layers and assumes no gaps or voids between continuum elements (Braja M.Das, 2010). Unlike the discrete approach, this approach can be applied for calculating the kinematic effect and simulation of dynamic pore water pressure in the soil.

2.1.2.1. The Reissner Model

The governing pressure-deflection equation is expressed at the interface between the foundation slab and the subgrade. This model places a foundation layer beneath the slab (Dutta and Roy, 2002). The model is based on the following assumptions:

(i) Stresses in the plane across the base layer are negligibly small.

(ii) The foundation layer's top and bottom surfaces have zero horizontal displacements.

The pressure-deflection relationship is expressed as follows.

$$C_1 w - C_2 \nabla^2 w = p - \frac{C_2}{4C_1} \nabla^2 p \tag{2.6}$$

$$C_1 = \frac{E}{H} \tag{2.7}$$

$$C_2 = \frac{HG}{3} \tag{2.8}$$

where p is a distributed load along the foundation, E, G are the foundation's elastic moduli, and H is the foundation layer's thickness. The H^2G/E term in Equation 2.6, also known as differential shear stiffness, allows for a higher level of agreement with actual soil behavior. One advantage of the model is to maintain the Winkler model's mathematical simplicity.

2.1.2.2. The Vlasov and Leont’ev Model

The Vlasov and Leont'ev (1966) study proposed a two-parameter model that overcomes this disadvantage of the Winkler model by using the variational method and taking the shear strains which occur due to the continuous structure of the soil into account. In this model proposed by the researchers, vertical displacements are calculated based on a parameter shown as γ. This γ parameter should not be confused with the unit weight of the soil or the shear strain symbols, which are frequently used in soil mechanics. Vallabhan and Das (1988) developed a method that allows this γ parameter to be calculated with an iterative approach. The differences between the Vlasov and Leont'ev (1966) and the Winkler (1867) can be briefly summarized as:

- In the Winkler model, the soil is modeled with discrete springs; therefore, the soil displacements in the system are limited by the length of the foundation in the x-direction as shown in Figure 2.2. This means that the continuous structure of the soil is ignored; hence, the actual deformation behavior cannot be obtained in the soil beyond the points where the foundation ends. To overcome this shortcoming of the Winkler model, new models which take the continuous structure of the soil into account have been developed by researchers such as Vlasov and Leont'ev (1966) and Nogami and Lam (1987).
- The Vlasov and Leont'ev (1966) explained the effect of shear-strain energy in the soil, which is neglected in Winkler (1867). This model considers shear forces which are due to the soil displacements on the beam endpoints (Dutta and Roy, 2002). In this context, it is a more realistic and better approach.

2.1.2.3. The Vallabhan and Das Model

The modified Vlasov model presented by Vallabhan and Das (1988, 1991a) is an iterative approach to employ the model proposed by Vlasov and Leont'ev (1966). The solution algorithm proposed in this model results in a compatible foundation deflection and soil displacement due to load on the foundation. However, they did not extend their interest to include soil nonlinearity.

Vallabhan and Das (1988) used the model shown in Figure 2.8 in their studies. Essentially, this model shows modeling of a continuous foundation of width ℓ as a beam on elastic soil and assuming plane strain conditions.

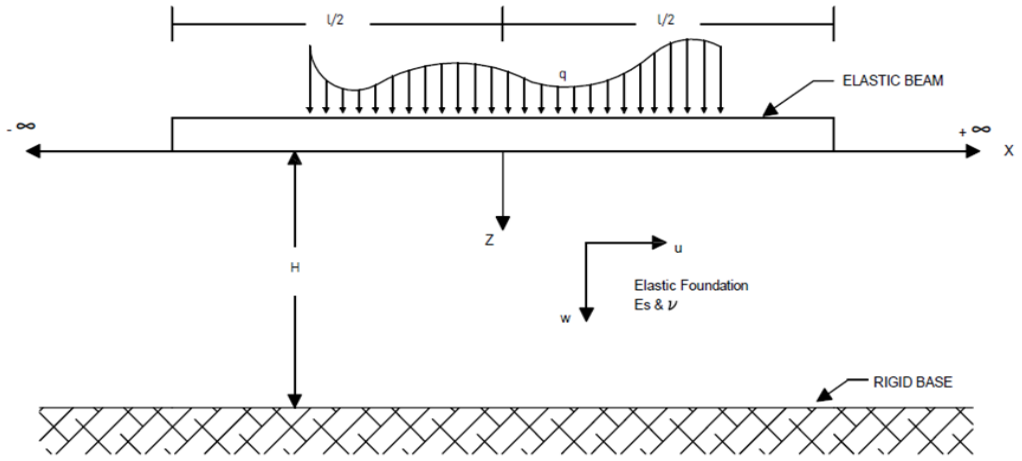

Figure 2.8. Representation of Vlasov model

(modified from Vallabhan and Das, 1988)

The minimum potential energy function in plane strain condition (Reddy, 1984) is expressed in the following equation.

$$\pi = \int_{-\ell/2}^{\ell/2} \frac{E_b I_b}{2}\left(\frac{d^2\overline{w}}{dx^2}\right)^2 dx + \int_{-\infty}^{\infty}\int_{0}^{H} \frac{b}{2}\left(\sigma_x\varepsilon_x + \sigma_z\varepsilon_z + \tau_{xz}\gamma_{xz}\right) dzdx - \int_{-\ell/2}^{\ell/2} q(x)\overline{w}dx \tag{2.9}$$

Here, E_b and I_b represent the beam's modulus of elasticity and moment of inertia, respectively; q is the vertical distributed load acting on the beam. Stresses that occur at any point in the foundation are calculated using constitutive relations and strain-displacement equations of elasticity.

$$\begin{Bmatrix}\sigma_x\\ \sigma_x\\ \tau_{xz}\end{Bmatrix} = \frac{E(1-\nu)}{(1+\nu)(1-2\nu)}\begin{pmatrix}1 & \nu/1-\nu & 0\\ \nu/1-\nu & 1 & 0\\ 0 & 0 & 1-2\nu/2(1-\nu)\end{pmatrix}\begin{Bmatrix}\partial u/\partial x\\ \partial w/\partial z\\ \partial u/\partial z + \partial w/\partial x\end{Bmatrix} \tag{2.10}$$

In Figure 2.8, the displacements in the soil of the foundation are shown by the following equations in the vertical and horizontal directions, respectively.

$$u(x,z)=0 \tag{2.11}$$

$$w(x,z)=\overline{w}(x)\phi(z) \tag{2.12}$$

Here *w* is the displacement of the beam along x-axis and in the z-direction, and $\phi(z)$ is the reduction function of the displacement. At this stage, *u* values, which are the displacement in the horizontal direction, have been neglected considering because they are assumed to be very small. After combining Equations 2.10, 2.11, and 2.12, Equation 2.9 has turned into Equation 2.13.

$$\pi=\int_{-\ell/2}^{\ell/2}\frac{E_bI_b}{2}\left(\frac{d^2\overline{w}}{dx^2}\right)^2dx+\frac{E_sb}{2}\int_{-\infty}^{\infty}\int_0^H\left[\frac{(1-\nu)}{(1+\nu)(1-2\nu)}\overline{w}^2\left(\frac{d\phi}{dz}\right)^2+\frac{1}{2(1+\nu)}\left(\frac{d\overline{w}}{dx}\right)^2\phi^2\right]dzdx-\int_{-\ell/2}^{\ell/2}q(x)\overline{w}dx \tag{2.13}$$

By using principles of variational calculus and placing $\overline{w}$ and ϕ in Equation 2.13, $\delta\pi$ is found as follows.

$$\delta\pi=\int_{-\ell/2}^{\ell/2}\frac{d^2}{dx^2}\left(E_bI_b\frac{d^2\overline{w}}{dx^2}\right)\delta\overline{w}dx-\int_{-\infty}^{\infty}2t\frac{d^2\overline{w}}{dx^2}\delta\overline{w}dx+\int_{-\infty}^{\infty}k\overline{w}\delta\overline{w}dx-\int_{-\ell/2}^{\ell/2}q(x)\delta\overline{w}dx+\int_0^H\left\{-m\frac{d^2\phi}{dz^2}+n\phi\right\}\delta\phi dz+\left[E_bI_b\frac{d^2\overline{w}}{dx^2}\delta\left(\frac{d\overline{w}}{dx}\right)-\frac{d}{dx}\left(E_bI_b\frac{d^2\overline{w}}{dx^2}\right)\delta\overline{w}\right]_0^{\ell}+m\left[\frac{d\phi}{dz}\delta\phi\right]_0^H+2t\left[\frac{d\overline{w}}{dx}\delta\overline{w}\right]_{-\infty}^{\infty}=0 \tag{2.14}$$

Here, *t* and *k* are the strength parameters of the soil and expressed as follows.

$$2t=\int_0^H\frac{E_sb}{2(1+\nu)}\phi^2dz \tag{2.15}$$

$$k=\int_0^H\frac{E_sb(1-\nu)}{(1+\nu)(1-2\nu)}\left(\frac{d\phi}{dz}\right)^2dz \tag{2.16}$$

ν seen in Equations 2.15 and 2.16 is the Poisson's ratio. For calculating coefficients of $\delta\overline{w}$, the following equations are used. First coefficient is for $-\ell/2 < x < \ell/2$ (for the beam).

$$\frac{d^2}{dx^2}\left(E_b I_b \frac{d^2\overline{w}}{dx^2}\right) - 2t\frac{d^2\overline{w}}{dx^2} + k\overline{w} = q(x) \tag{2.17}$$

After applying boundary conditions: $x = -\ell/2, \ell/2$ in Equation 2.17 the following equations, Equation 2.18 and Equation 2.19 are obtained.

$$E_b I_b\left(\frac{d^2\overline{w}}{dx^2}\right)\delta\left(\frac{d\overline{w}}{dx}\right) = 0 \tag{2.18}$$

$$\left[\frac{d}{dx}\left(E_b I_b \frac{d^2\overline{w}}{dx^2}\right) - 2t\frac{d\overline{w}}{dx}\right]\delta\overline{w} = 0 \tag{2.19}$$

Second coefficient is for $-\infty < x < -\ell/2$ *and* $\ell/2 < x < +\infty$ (for the foundation).

$$-2t\frac{d^2\overline{w}}{dx^2} + k\overline{w} = 0 \tag{2.20}$$

After applying boundary conditions: $x = -\infty, -\ell/2$ *and* $x = \ell/2, \infty$ in Equation 2.20 the following equation, Equation 2.21 is found.

$$E_b I_b\left(\frac{d^2\overline{w}}{dx^2}\right)\delta\left(\frac{d\overline{w}}{dx}\right) = 0 \tag{2.21}$$

For calculating coefficients of $\delta\phi$, Equation 2.22 is used.

$$-m\frac{d^2\phi}{dz^2} + n\phi = 0 \tag{2.22}$$

The solution parameter is γ, it is expressed as follows.

$$\left(\frac{\gamma}{H}\right)^2 = \frac{n}{m} = \frac{1-2\nu}{2(1-\nu)}\frac{\int_{-\infty}^{\infty}\left(\frac{d\overline{w}}{dx}\right)^2 dx}{\int_{-\infty}^{\infty}\overline{w}^2 dx} \tag{2.23}$$

The reduction function takes the value $\phi(0)=1$ on the lower face of the foundation and continues decreasing, and it is accepted as $\phi(H)=0$ on the lower face of the soil and is obtained with these following equations.

$$\frac{d^2\phi}{dz^2} - \left(\frac{\gamma}{H}\right)^2\phi = 0 \tag{2.24}$$

$$\left[\frac{d\phi}{dz}\delta\phi\right]_0^H = 0 \tag{2.25}$$

$$\phi(z) = \frac{\sin\gamma\left(1-\frac{z}{H}\right)}{\sinh\gamma} \tag{2.26}$$

Vallabhan and Das (1991a) express new values of *k* and *t* derived from 2.15 and 2.16 respectively with using Equation 2.26. They expand the $\left(\frac{\gamma}{H}\right)^2$ ratio with these equations and created the finite difference model to solve differential Equation 2.17. These equations 2.27 and 2.28 are expressed as follows.

$$k = \frac{b(1-\nu)}{8H(1+\nu)(1-2\nu)}\left[\frac{E_1(2\gamma\sinh 2\gamma + 4\gamma^2) + (E_2 - E_1)(\cosh 2\gamma - 1 + 2\gamma^2)}{\sinh^2\gamma}\right] \tag{2.27}$$

$$2t = \frac{bH}{16\gamma^2(1+\nu)}\left[\frac{E_1(2\gamma\sinh 2\gamma - 4\gamma^2) + (E_2 - E_1)(\cosh 2\gamma - 1 - 2\gamma^2)}{\sinh^2\gamma}\right] \tag{2.28}$$

The new $\left(\frac{\gamma}{H}\right)^2$ ratio to solve deflection of the beam is found as follows.

$$\left(\frac{\gamma}{H}\right)^2 = \frac{(1-2\nu)}{2(1-\nu)}\frac{\int_0^L\left(\frac{d\overline{w}}{dx}\right)^2 dx + \frac{1}{2}\sqrt{\frac{k}{2t}\left[\overline{w}^2(0) + \overline{w}^2(\ell)\right]}}{\int_0^L \overline{w}^2(x)\,dx + \frac{1}{2}\sqrt{\frac{2t}{k}\left[\overline{w}^2(0) + \overline{w}^2(\ell)\right]}} \tag{2.29}$$

In finite difference model, the Equation 2.30 is obtained by for every node *i* in domain by using central difference method.

$$w_{i-2} - (4+\alpha)w_{i-1} + (6+2\alpha+\beta)w_i - (4+\alpha)w_{i+1} + w_{i+2} = \frac{q_i h^4}{E_b I_b} \tag{2.30}$$

α and β are calculated using the equations given below.

$$\alpha = \frac{2th^2}{E_b I_b} \tag{2.31}$$

$$\beta = \frac{kh^4}{E_b I_b} \tag{2.32}$$

Here, $h = \ell/N$, and *N* is the number of nodes used in the finite-difference model. For the nodes at the end of the beam, they used modified equations from Equation 2.30 which

include boundary conditions. These finite difference equations are developed for the right-hand side end of the beam at the nodes *n* and *n-1* and they are obtained as follows.

$$w_{n-3}-(4+\alpha)w_{n-2}+(5+2\alpha+\beta)w_{n-1}-(2+\alpha)w_n=\frac{q_{n-1}h^4}{E_bI_b}+\frac{\widetilde{M}_n h^2}{E_bI_b} \tag{2.33}$$

$$w_{n-2}-(2+\alpha)w_{n-1}+\left(1+\alpha+\frac{\beta}{2}+\sqrt{2kt}\,\frac{h^3}{EI}\right)w_n=\frac{q_n h^4}{2E_bI_b}-\frac{\widetilde{M}_n h^2}{E_bI_b}+\frac{\widetilde{Q}_n h^3}{E_bI_b} \tag{2.34}$$

where $\widetilde{M}_n$ is the bending moments and $\widetilde{Q}_n$ is the shear forces at the end of the beam.

Vallabhan and Das (1988, 1991a) study can be summarized as follows:

1) ϕ values are calculated by assuming a γ value.
2) *t* and *k* values are calculated by using ϕ.
3) With the *t* and *k* values found, *w* is recalculated.
4) Based on the *w* values found, the γ value is recalculated.
5) The γ in step 4 is compared with the γ values in step 1, if the difference is less than a specified tolerance value, the obtained *w* values are accepted as the solution, assuming it converges to the solution.
6) If the difference calculated in step 5 is greater than the desired tolerance value, a new ϕ is calculated using the γ values in step 4, and the above steps are repeated until convergence is achieved by continuing from step 2.

This method and the later studies following the approaches arising from this method have been frequently used by researchers in soil-structure interaction problems such as modeling the behavior of various foundations under dynamic or static loads (Sun, 1994; Aşık, 1999; Isbuga, 2020).

2.2. Modulus Reduction Curves

Laboratory tests have shown that soils exhibit linear elastic behavior only at small strain values. In Figure 2.9 (a) the shear modulus (initial shear modulus) corresponding to the small values of shear strain (ε_s), at the initial stage of loading is displayed as the highest

shear modulus value ($G_0=G_{max}$) while the secant modulus is defined as the slope of the line connecting the origin of shear stress axis and the shear stress value at the corresponding a certain shear strain value on the hyperbolic curve. The secant modulus decreases in a certain way as it follows the asymptote of the hyperbolic curve at high strain value due to the shape of the hyperbolic curve. As the deformations increase, the stress-strain behavior for various soils will move away from the linear elastic behavior and this phenomenon can be depicted with a hyperbolic curve. G_{max} and τ_{max} (maximum shear stress) values are sufficient to express the behavior of soils under shear with a hyperbolic stress-strain curve in the simplest way (Hardin and Drnevich, 1972a;1972b). For loads where deformations exceed small strain values, it will not be possible to use the initial shear modulus. Hence, the initial shear modulus must be reduced based on the current shear stress/strain values. The initial shear modulus of undisturbed soil samples under shear load can be taken equal to the secant modulus ($G=G_{max}$) at low strain values. Therefore, the ratio of G/G_{max} = 1 at the beginning of the loading and it also decreases accordingly as shown in Figure 2.9 (b).

For curves of E/E_{max} change due to axial strain (ε_a), E_{max} initial modulus of elasticity (maximum modulus of elasticity) is defined as the modulus of elasticity at small axial strains ($E_{max} = E$), and E is the secant modulus of elasticity corresponding to that value at any strain value. Therefore, a curve similar to the one shown in Figure 2.9 (a) can also be obtained for the stress-strain curve under axial load shown (Fahey and Carter, 1993).

Although the hyperbolic curve is not suitable for modeling the failure or post-failure behavior of dense sands and OC clays, it can be used for small to intermediate strain leves that will be the interest of our foundation deflection problems. In cases where the foundation designs are not expected to serve at strain values close to failure (by taking measures such as changing the foundation design, etc.) depending on the reduction of the E or G values, this method can be applied to determine the foundation deflection.

The reduction due to these shear strain or axial strain values must be considered in the analysis to obtain a realistic behavior. The critical point here is that since the strain or the stage of stress is not known from the beginning, it cannot be determined how much the soil strength modulus will be reduced; therefore, the value of the reduced soil strength modulus in the calculations should be solved depending on the strain or stress values that will occur.

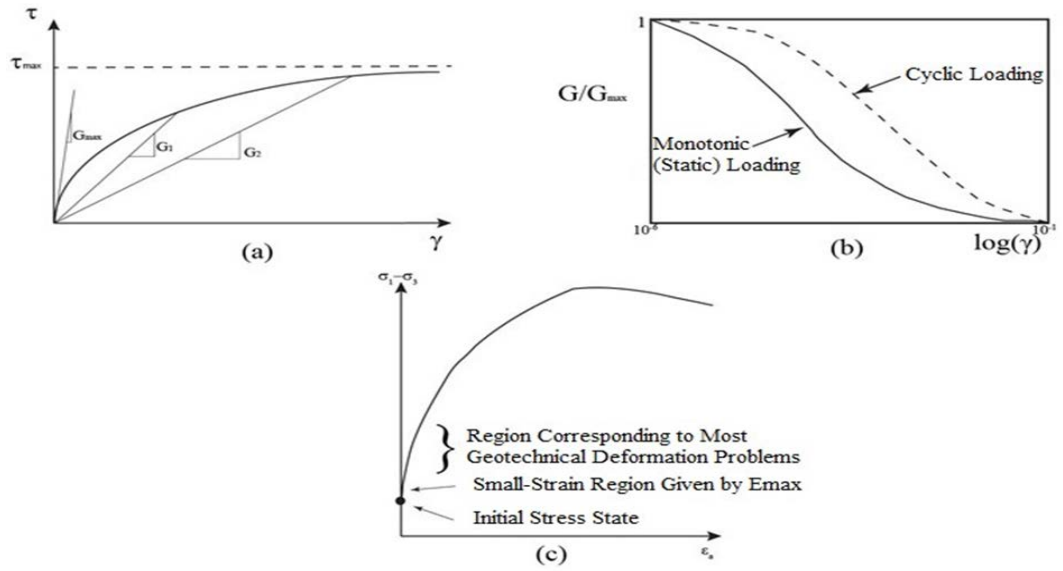

Figure 2.9. (a) Definitions of representative shear stress-strain, G_{max} and G_{sec} (b) Variation of representative shear modulus reduction with respect to logarithmic shear strain for static and cyclic loadings (c) Figurative representation of the modulus of elasticity to be obtained from triaxial compression test and geotechnical problems application ranges

(modified from Mayne and Schneider, 2001)

The soil strength reduction method proposed in this study has been applied to some geotechnical problems. G/G_{max} curves obtained from dynamic cyclic experiments were determined for different soils and used to calculate the behavior of horizontal soil layers under dynamic loads (Shnabel et al., 1972; Kokoshu, 1980; Seed et al., 1986; Ishibashi and Zhang, 1993). The SHAKE program (Shnabel et al., 1972), which is frequently used in this field, reduces the G/G_{max} values with an iterative method according to the strains obtained. The reduction in shear modulus or modulus of elasticity can also be used in geotechnical calculations subjected to static loads (Fahey and Carter, 1993; LoPresti et al.,1993,1995), and studies that consider the reductions in modulus of elasticity and shear modulus under such static loads can be explained in this context for pile foundations (Mayne & Schneider, 2001; Niazi & Mayne, 2014).

Niazi and Mayne (2014) applied a method that reduces the G/G_{max} values according to the stress values formed in the analysis of a pile foundation. Fahey and Carter (1993) showed that a similar curve to the G/G_{max} curve previously shown under dynamic cyclic loads can be found for static monotonic loading and observed that the G/G_{max} curve decreases more sharply under static monotonic loading shown in Figure 2.9 (b). As

mentioned above, E/E_{max} curves can also be used, since a similar behavior curve to the hyperbolic shear stress-strain behavior will be seen in the uniaxial stress-strain behavior. Tatsuoka and Shibuya (1992) and Lo Presti et al. (1993,1995) showed that the approach used for G/G_{max} is also valid for Young's modulus and how E/E_{max} values decrease due to strain in different types of soils.

CHAPTER 3

NUMERICAL METHODOLOGY

As stated in Chapter 2, Vallabhan and Das (1988, 1991a) proposed and implemented an algorithm that uses Equation 2.13 and Equation 2.23 obtained from the Vlasov model and enables the γ value to be determined by an iterative method. This algorithm first includes the determination of the foundation displacement and then the calculation of the γ parameter with the results obtained. Then, if the difference between the γ values obtained in two successive iterations is less than the specified tolerance value, the solution is considered as converged and the results are calculated for the total load. However, this algorithm and formulation will be insufficient when the nonlinear behavior of the soil is considered. Such an algorithm has not been developed before for the soil-structure interaction model and it is anticipated to be used in this study. Since it would be invalid to assume a constant Young's modulus value at every point of the soil due to nonlinear behavior, the soil strength parameters should be modified to take this behavior into account. In this study, these strength parameters *t* and *k* are calculated by using Equation 2.15 and Equation 2.16 by numerical solution instead of Equation 2.27 and Equation 2.28. The total load should be divided into loading steps, and the reduced soil parameters should be used depending on the strain value formed in each step, and the soil strength parameters should be recalculated over these reduced parameters. Therefore, it is necessary to add another algorithm that considers the nonlinear behavior of the soil. After obtaining converged results in each loading step, the load can be increased and the next loading step can be started. With this approach proposed in this study, the decrease in soil parameters will be included in the analysis.

3.1. Model

In the previous studies of Vallabhan and Das (1988, 1991a), the researchers proposed coupled differential equations for the foundation deflection and soil displacements and also presented a solution algorithm. The focus of this section is to explain how this model,

which was previously developed by assuming the soil as a linear material under vertical loads, can be developed to account for a more realistic soil behavior by using modulus reduction curves. Such curves can be determined by conducting standard soil mechanics experiments. For example, representative soils samples can be taken from soil layers at construction sites. Then, direct shear tests can be conducted on these samples to provide the shear load-deformation curves for each layer. After the shear stress-strain curves are determined for each layer separately, the maximum shear moduli for layers are obtained by calculating the slope of the curves at small strain ($<10^{-6}$) or by following the various methods given in the literature for different soil types such as the work by Fahey and Carter (1993). Then, the secant modulus values at varying shear strain levels can be calculated as shown in Figure 2.9 (a). As a result, the modulus reduction curves for each layer will be available to be used as material inputs.

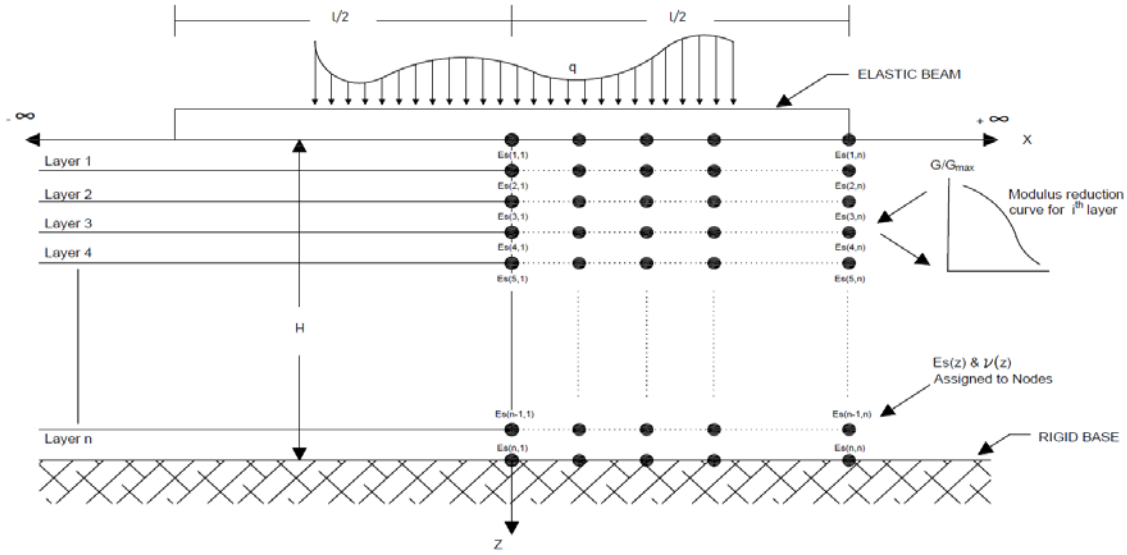

Figure 3.1. Foundation and loading model on continuous soil

Accordingly, in the present study: the mathematical formulation was changed and a new algorithm was developed so that the nonlinear behavior of the soil layer can be considered. Then, a Fortran code was developed for the analysis of the foundation under static loads in the vertical direction. Secondly, the multiple analysis of the foundation under static loads in the vertical direction were carried out with the new approach. With this approach, layering in the soil can be achieved by assigning different Young's (Elasticity) modulus and Poisson's ratio to each layer. As shown in Figure 3.1, although

all the nodes have the same initial modulus at the same depth level, once the loading causes nonlinear deformations at these nodes, their modulus value will be different depending on their strain level. This is achieved by creating nodes along the z and x-axis then assigning different material parameters to these nodes. Thus, a soil profile that is not homogeneous along the z-axis and consists of different layers with nonlinear soil behavior is considered. Therefore, the displacements that occur in the foundation and the soil under the foundation is modeled more realistically.

To include strain-dependent modulus reduction, the following equations were modified. The new equations take care of the pointwise strain change and modulus reduction in the discretized domain.

$$2t_i = \int_0^H \frac{E_{s_i} b}{2(1+\nu)} \phi^2 dz \cong \sum_{n=1}^{N} \frac{E_{n_i} b}{2(1+\nu)} {\phi_n}^2 \Delta z \tag{3.1}$$

$$k_i = \int_0^H \frac{E_{s_i} b(1-\nu)}{(1+\nu)(1-2\nu)} \left(\frac{d\phi}{dz}\right)^2 dz \cong \sum_{n=1}^{N} \frac{E_{n_i} b(1-\nu)}{2(1+\nu)(1-2\nu)} \left(\frac{\phi_{n+1}-\phi_n}{\Delta z}\right)^2 \Delta z \tag{3.2}$$

$$\left(\frac{\gamma}{H}\right)^2 = \frac{(1-2\nu)}{2(1-\nu)} \frac{\sum_{i=1}^{n} \left(\frac{\bar{w}^2{}_{i+1} - \bar{w}^2{}_i}{\Delta x}\right)^2 + \frac{1}{2}\sqrt{\frac{k_n}{2t_n}\left[\bar{w}^2(0) + \bar{w}^2(\ell)\right]}}{\sum_{i=1}^{n} \bar{w}^2{}_i \Delta x + \frac{1}{2}\sqrt{\frac{2t_n}{k_n}\left[\bar{w}^2(0) + \bar{w}^2(\ell)\right]}} \tag{3.3}$$

Equation 2.17 can be expanded by using the finite difference formulation. However, this time, the equations include the modified k_i and $2t_i$ parameters as shown below:

$$\alpha_i = \frac{2t_i h^2}{E_b I_b} \tag{3.4}$$

$$\beta_i = \frac{k_i h^4}{E_b I_b} \tag{3.5}$$

$$w_{i-2} - (4+\alpha_i) w_{i-1} + (6 + 2\alpha_i + \beta_i) w_i - (4+\alpha_i) w_{i+1} + w_{i+2} = \frac{q_i h^4}{E_b I_b} \tag{3.6}$$

$$w_{n-3}-\left(4+\alpha_{n-1}\right)w_{n-2}+(5+2\alpha_{n-1}+\beta_{n-1})w_{n-1}-\left(2+\alpha_{n-1}\right)w_n=\frac{q_{n-1}h^4}{E_bI_b} \tag{3.7}$$

$$+\frac{\widetilde{M}_n h^2}{E_bI_b}$$

$$w_{n-2}-\left(2+\alpha_n\right)w_{n-1}+\left(1+\alpha_n+\frac{\beta_n}{2}+\sqrt{2k_nt_n}\,\frac{h^3}{EI}\right)w_n=\frac{q_nh^4}{2E_bI_b}-\frac{\widetilde{M}_n h^2}{E_bI_b}+\frac{\widetilde{Q}_n h^3}{E_bI_b} \tag{3.8}$$

where *i* represents the node number in *x*-direction, *Δz* is the distance between two nodes in the *z*-direction, *N* is the number of nodes in *z*-direction and E_{n_i} is the E_{new} value that corresponds to the node. Assumptions made in this study are as given:

- It was assumed that the same differential equation for the decay function ϕ, which is calculated with Equation 2.26, governs in the vertical direction as Vallabhan and Das (1991a) proposed.
- When the calculations hit the nonlinear range, it will result in different soil elasticity modulus at different nodes depending on the strain level reached at that individual node. Such changes will yield a variation of soil parameters, which are different from the initial case, along the beam length in the x-direction. For the sake of mathematical simplicity, we follow the same differential equation proposed for the initial case.
- The strains calculated using the displacement assumptions given in Equation 2.11 and Equation 2.12 are expressed as

$$\varepsilon_z=\frac{dw}{dz} \tag{3.9}$$

$$\varepsilon_{zx}=\frac{dw}{dx}+\frac{du}{dz} \tag{3.10}$$

  Since the plane strain conditions are held, *du/dz=0* in Equation 3.10, only the remaining term contributes to the shear strain used in the iterations. For the E/E_{max} curves, ε_z values are used as the corresponding strain.

The reduced Young's moduli and shear moduli at nodes are calculated based on the experimental or hypothetical E/E_{max} or G/G_{max} curves and the strain values. When analytical expressions are not available for modulus reduction curves, we can introduce reduction values and corresponding shear strain values in a tabulated form. Hence, another algorithm is implemented to calculate the new modulus reduction value for a given strain value in the tabulated form. First, the strain values are sorted in ascending

order in which the calculated strain can be fit in between two consecutive strain values in order. The calculated strain values' exact position within this range is obtained by the program and the E/E_{max} or G/G_{max} value corresponding to this range is used for E_{new} calculation. Thus, the precise E_{new} is obtained for this exact strain value instead of an approximate E value that can be obtained by considering the average of the chosen range limits. This phenomenon can also be observed in Figure 3.2 as the calculated strain value is given between any strain$_{(i)}$ and strain$_{(i+1)}$ value in its exact position. G_{new} *or* E_{new} values are calculated by Equation 3.11.

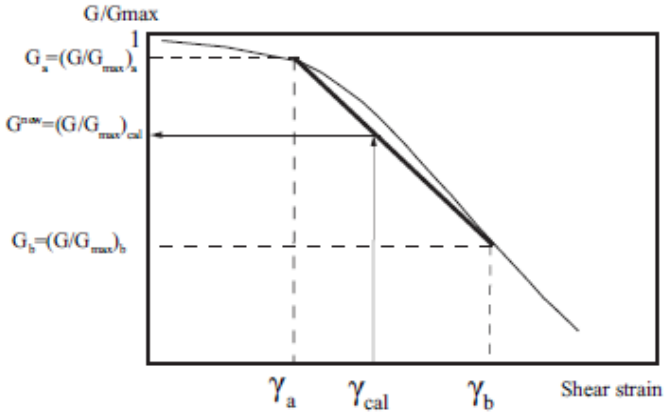

Figure 3.2. Shematic representation of calculation of new G_{new} or E_{new} based on the calculated strain

$$G_{new} = \frac{\left(\left(\frac{x}{y}\right) * G_a + G_b\right) * \left(G_{\max}\right)}{\left(1 + \left(\frac{x}{y}\right)\right)} \tag{3.11}$$

where $x = \gamma_{cal} - \gamma_a$ and $y = \gamma_b - \gamma_{cal.}$ The converged G_{new} or E_{new} values are used to calculate the new k_i and t_i values.

3.2. Algorithm

In this study, the reduction of either of the E/E_{max} or G/G_{max} curves according to the strain values is considered in the foundation analysis. However, the creation of these curves is

out of the scope of this study instead the curves given in the literature are taken into account. By using these curves, a solution and a program is obtained. The written program is designed to allow the use of either of the E/E_{max} and G/G_{max} curves, depending on the user's request. In addition, different values can be given for different layers or E/E_{max} curves can be given for one layer while G/G_{max} curves can be used for another layer. Thus, the program allows the modeling of different soils and experiments on the soils and offers more options to the user.

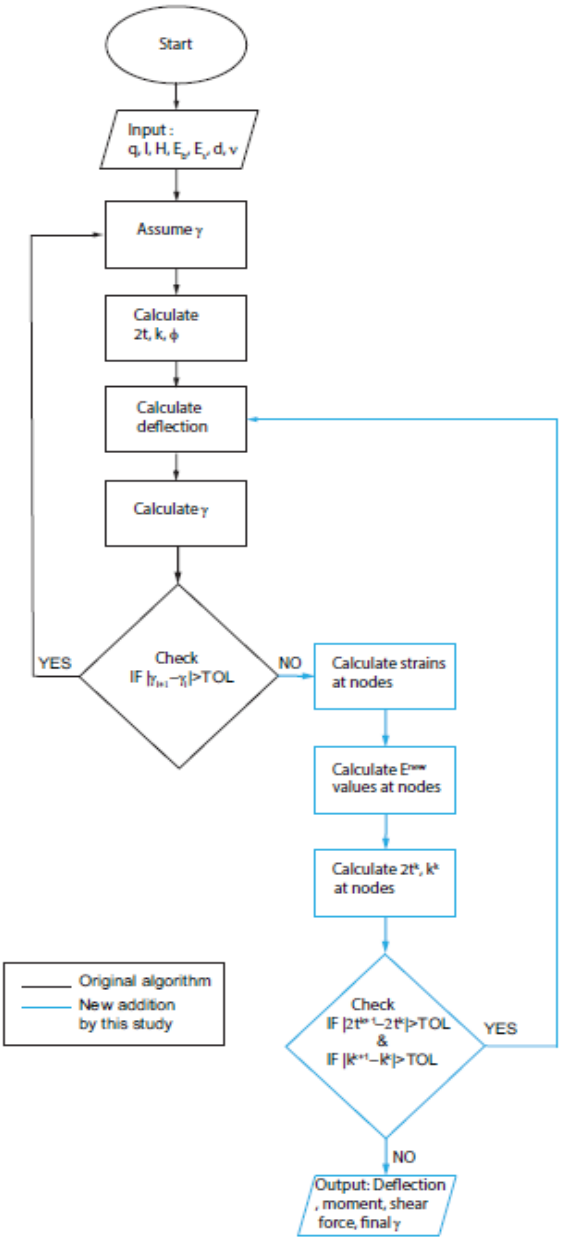

Figure 3.3. Algorithm for solving the problem

The key point at this stage is the development of an algorithm that incorporates the E/E_{max} or G/G_{max} curves. E_{max} and G_{max} values can be obtained by field or laboratory experiments, after the determination of reduction curves their reduced values can be included into the *t* and *k* parameter calculations. These *t* and *k* parameters, which show the strength of the soil, are reduced according to the strain values to occur. Thus, it considers the nonlinear decrease in the soil strength. The algorithm summarizing this approach is given in Figure 3.3. To include the nonlinear soil behavior, new additions to the algorithm introduced by Vallabhan and Das (1988, 1991a) are done. Firstly, the total applied load is divided into steps so that the total load is applied incrementally. When convergence is achieved at each load step, the result corresponding to that load step is used in the calculations of that step. Then, the load is increased and passed on to the next load step and the same steps are followed until the total load is reached. In this algorithm, the shear modulus or Young's (Elasticity) modulus of the soil at each node and Poisson's ratio are assigned to the solution points with the changes in their formulation. These initially assigned values are then reduced depending on the strains that occur, following the algorithm given in Figure 3.3. Hence, a nonlinear solution is obtained in this algorithm.

The algorithm given in Figure 3.3 can be explained as follows:

1. Number of loading steps is determined.
2. An initial value of γ is accepted.
3. ∅ values are calculated based on γ values.
4. *t* and *k* values are calculated by using ∅ values.
5. *w* values are obtained considering values obtained in step 4.
6. γ value is recalculated based on *w* values.
7. If the difference between the γ values found in steps 3 and 6 is greater than the specified tolerance, the steps are repeated starting from the step 3. If the desired tolerance is achieved, strain values are calculated at each point.
8. According to the calculated strain values, new *E* or *G* values are found for each point using E/E_{max} or G/G_{max} curves.
9. The *t* and *k* parameters are recalculated using the new *E* or *G* and new w values assigned to the nodes. These new *t* and *k* values obtained by Equation 3.1 and Equation 3.2 are compared with the *t* and *k* parameters found in step 4. If the

difference between the t and k values in both steps is greater than the desired tolerance, the calculations are repeated according to the new soil parameters by going to the 6^{th} step.

10. If the tolerance conditions on γ and soil parameters t and k are both met in the same iteration, the solution is considered converged and the result is found for the current load step.
11. The load is increased and passed on to the next loading step.

CHAPTER 4

RESULTS AND DISCUSSIONS

In this Chapter, the examples given in Vallabhan and Das (1988, 1991a) are examined using the model and algorithm presented in Chapter 2 and a comparison with the finite element method (FEM) is also presented. The main purpose of solving these examples is to show the operability of the created algorithm.

The samples are compared using both the algorithm given in Vallabhan and Das (1988, 1991a) and the algorithm developed in this project. These examples have been applied for each value of the parameter M (E_2/E_1) which is found by taking the ratio of the elasticity modules at the top and bottom of the soil. Beam's features and dimensions are kept the same with the ones used in previous studies of Vallabhan and Das (1988, 1991a) and the algorithm presented in this study.

The modeled beam is given in Figure 4.1. The dimensions of the beam are considered as follows: length of the beam (L) = 30 m, width of the beam (b) = 1 m, depth of the beam (d) = 1 m. Modulus elasticity of the beam assumed as 10 GPa and modulus elasticity of the soil for loose Toyoura sand and dense Toyoura sand data taken from Teachavorasinskun et al. (1991).

Poisson's ratio of the soil layer is taken as 0.2 and uniformly distributed load is assumed as q = 100 kN/m for all examples except for the finite element method in which q = 25 kN/m. The soil depth (H) is considered as 15 m. These values are kept the same for all examples in this chapter.

The M (E_2/E_1) parameter have been used differently for each as M = 1 and 2. As stated in Chapter 3, E/E_{max} or G/G_{max} curves are entered into the program and nonlinear behavior is achieved by decreasing the strength parameters. The results obtained are explained using detailed plots in the following sections.

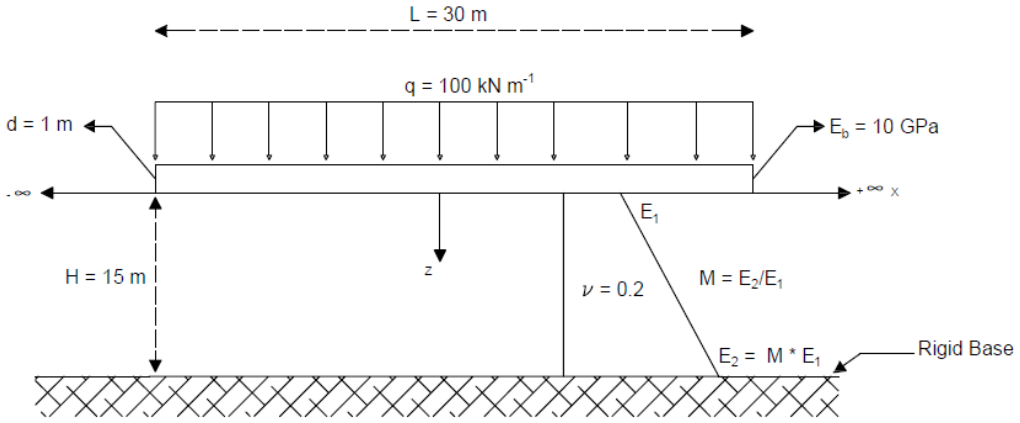

Figure 4.1 The model of the problems

(modified from Vallabhan and Das, 1991a)

4.1. The Reduction Curves Used in the Numerical Examples

Different G/G_{max} curves can be entered into the program because the developed algorithm enables the use of different types of soil properties obtained from the experiments for different soil layers. Thus, the results of nonlinear behavior on different types of soils can be examined. In these examples, loose Toyoura sand and dense Toyoura sand data taken from Teachavorasinskun et al. (1991) are used. Hence, the effect of different soil types on the response of the foundation deflection can be investigated. Data points in Teachavorasinskun et al. (1991) and curves used in the program are shown in Figure 4.2 and Figure 4.3.

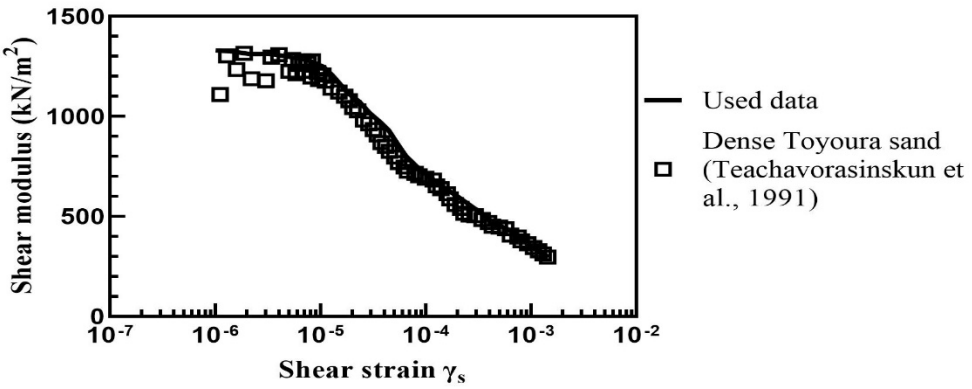

Figure 4.2 Used data of dense Toyoura sand

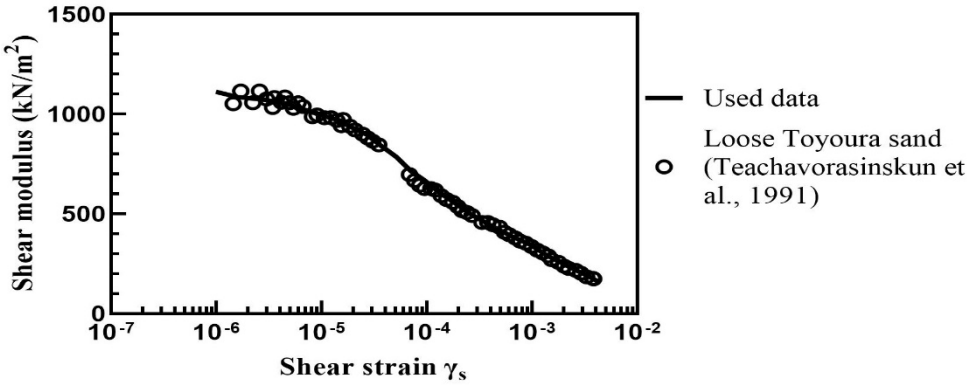

Figure 4.3 Used data of loose Toyoura sand

As seen in Figure 4.2 and Figure 4.3, curves are obtained for both sand types by considering the real data. The solid lines given in Figure 4.2 and Figure 4.3 show the fitted line used in the problems are solved by entering the obtained shear modulus curves into the program.

4.2. Example 1: Verification of the New Algorithm

In this section, the algorithm presented in this study was compared to the algorithm given in Vallabhan and Das (1991a) by solving a linear problem. The purpose of solving this example is to show that the algorithm developed in this study gives the same results as the method given in Vallabhan and Das (1991a) in case of linear problems.

In this comparison, the value of M has been taken as 1 and G/G_{max} values fed into the program have been taken as 1 throughout the entire soil for linearity. The model used is shown in Figure 4.4.

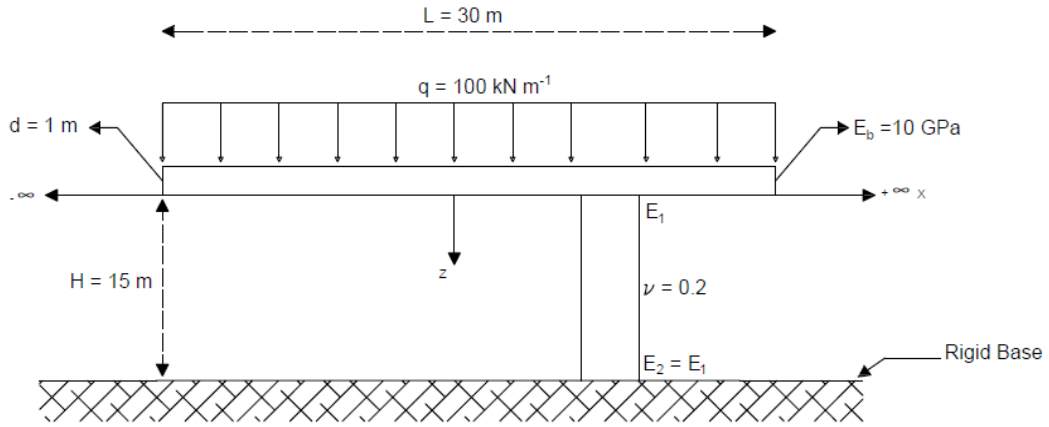

Figure 4.4 The model of the linear problem

(modified from Vallabhan and Das, 1991a)

N is the number of nodes in the discretized model and was taken as 30 and 40 in this example. The results with different number of *N* values showed that the results are not affected by number of nodes used in z-direction. Thus, the results obtained according to the number of different layers are compared with the results obtained from author's algorithm. The results obtained are given in Figure 4.5.

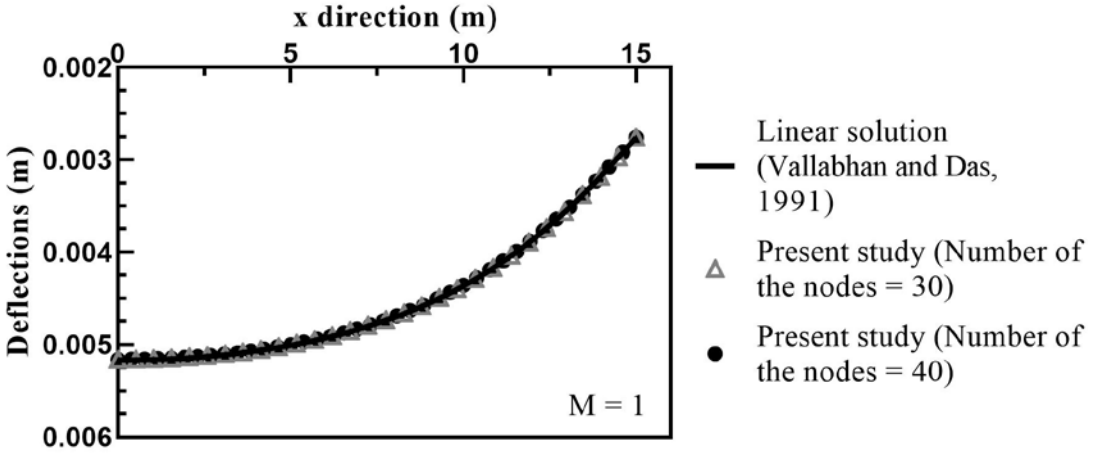

Figure 4.5 Comparison of linear deflections

As seen in Figure 4.5, the algorithm developed in this study and the previous algorithm gave very similar results for a different number of nodes (N). Thus, the accuracy of the developed algorithm for linear analysis has been demonstrated. Matching results proved that the algorithm works well when it is reduced back to the linear behavior.

Linear and nonlinear deflection results for M = 1 and 2 of loose Toyoura sand and dense Toyoura sand are compared by using Figure 4.6 and Figure 4.7.

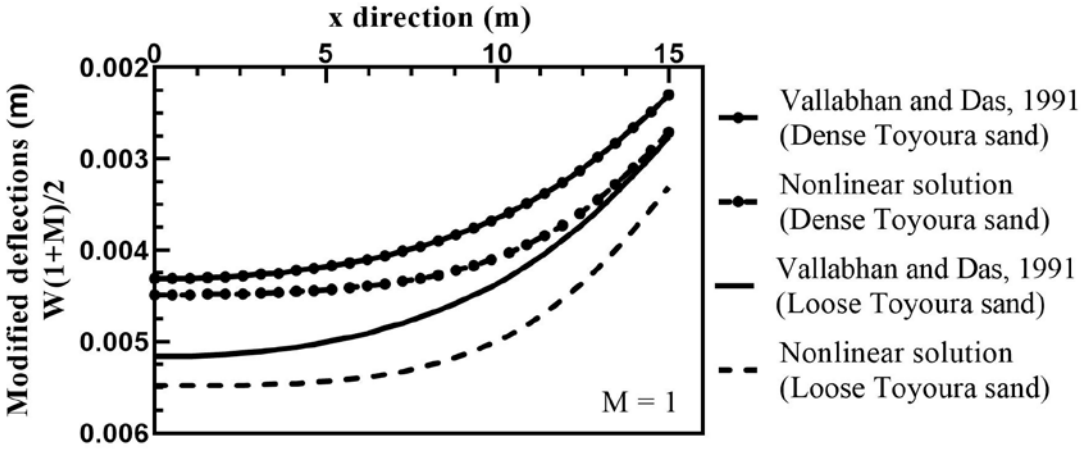

Figure 4.6 Modified deflection results for M = 1

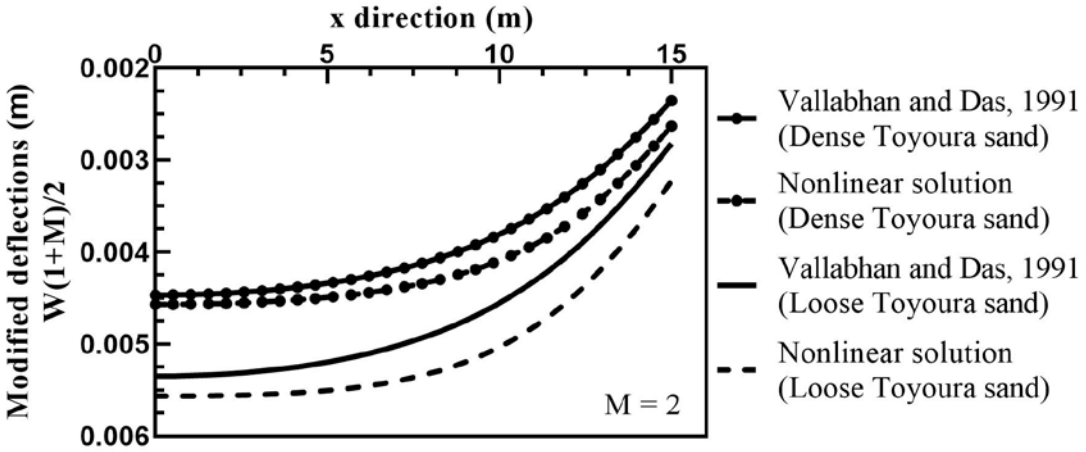

Figure 4.7 Modified deflection results for M = 2

As can be seen from the figures, loose Toyoura sand gave higher deflection values than dense Toyoura sand. For different M values, linear, loose Toyoura sand and dense Toyoura sand modified deflection values are obtained. The modified deflection values used here are calculated by multiplying the actual deflection values by $(1+M)/2$.

It has been observed that the resulting deflections are higher than those of linear solutions due to the decrease in the strength parameters in the nonlinear solutions. Also, the loose Toyoura sand values are higher than those of the dense Toyoura sand. This result shows the foundation effect of the G/G_{max} curve values on the response.

The bending moment values are obtained for each *M* value as well. These comparisons are shown in Figure 4.8 and Figure 4.9.

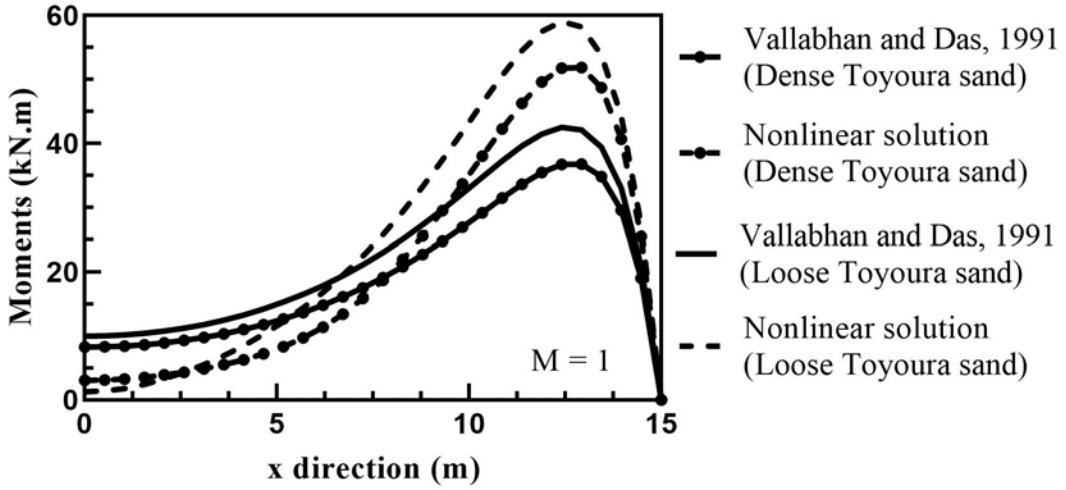

Figure 4.8 Bending moment results for M = 1

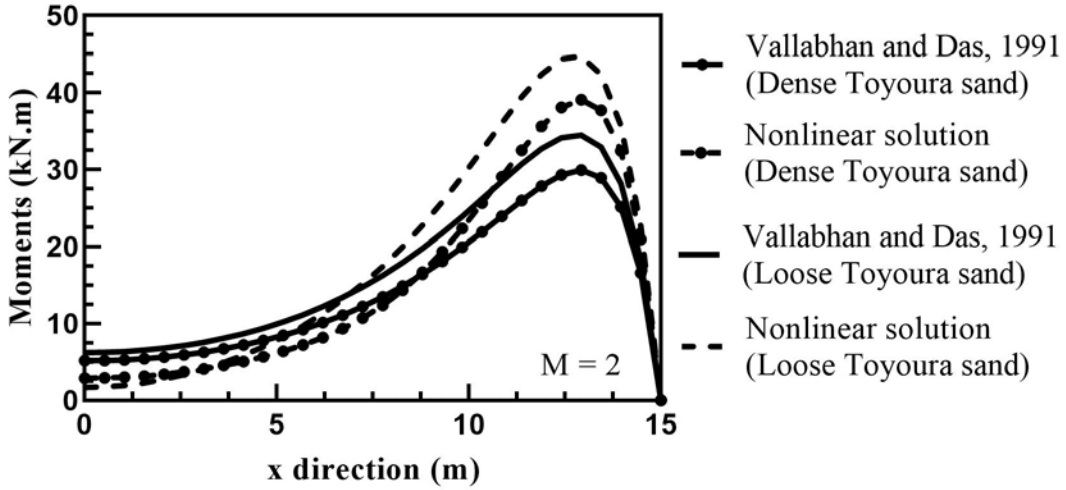

Figure 4.9 Bending moment results for M = 2

As it is shown in the figures, the nonlinear bending moment values are higher than the linear bending moment values. This is also a significant outcome of the proposed method presenting the effect of the use of the non-linear approach for the foundation analysis in the modified Vlasov model, even though peak value differs with soil type.

Lastly, the shear force distributions are obtained by using different *M* values for linear, dense Toyoura sand and loose Toyoura sand. These values are shown in Figure 4.10, Figure 4.11, Figure 4.12 and Figure 4.13.

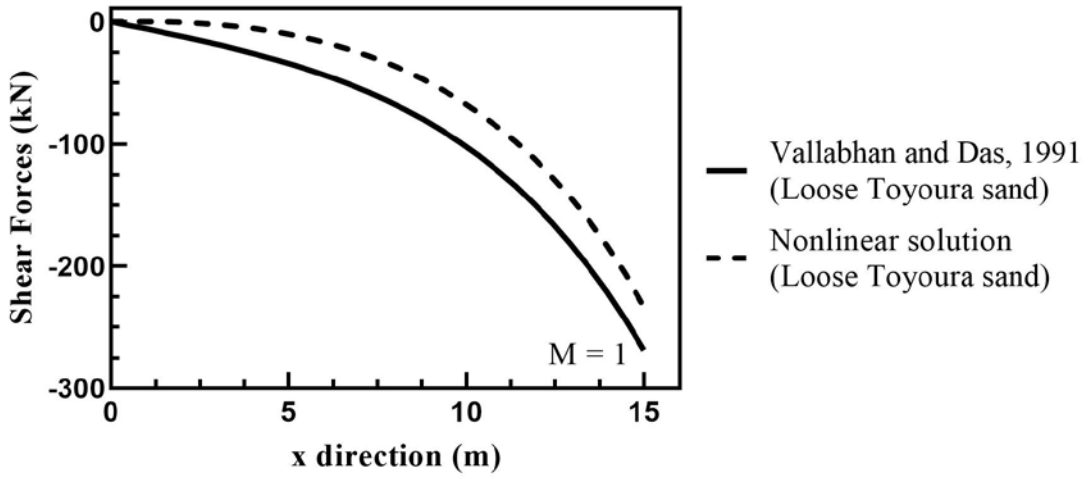

Figure 4.10 Loose Toyoura sand shear force results for M = 1

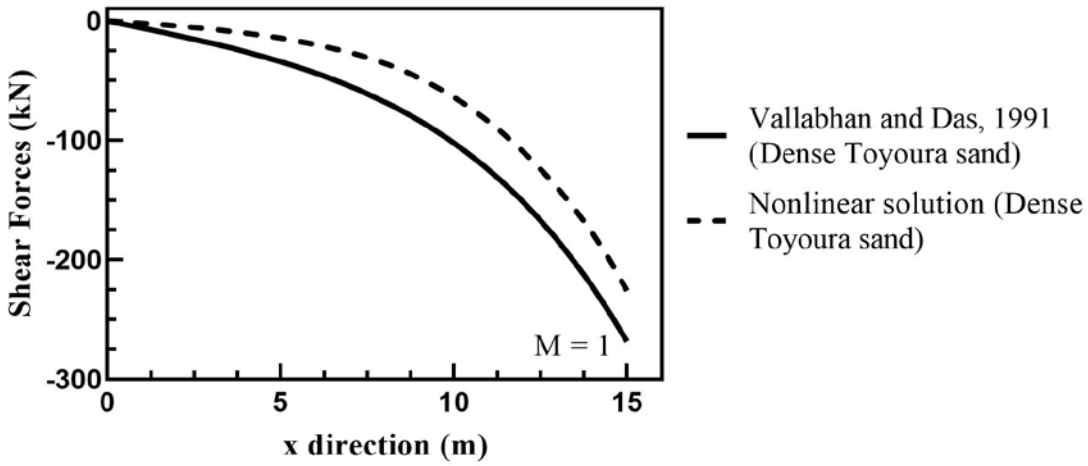

Figure 4.11 Dense Toyoura sand shear force results for M = 1

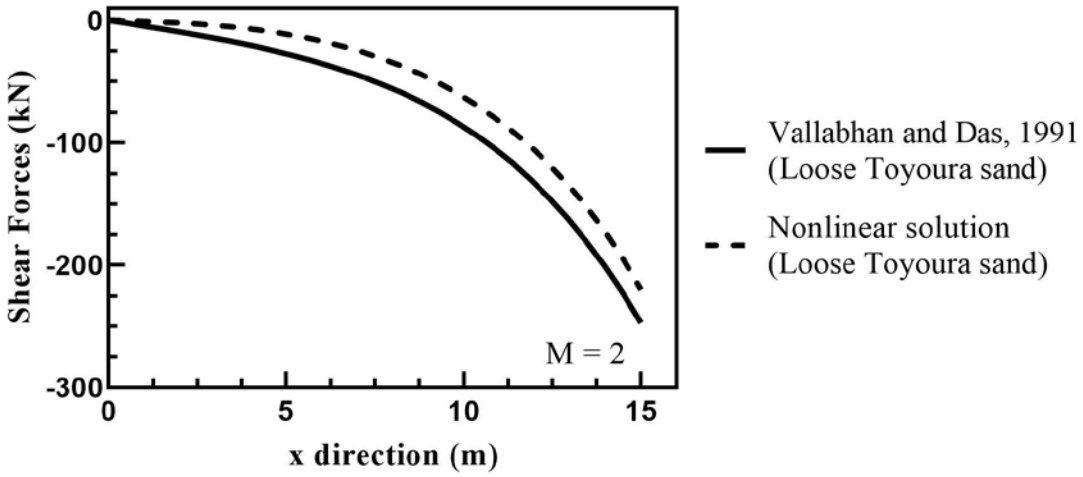

Figure 4.12 Loose Toyoura sand shear force results for M = 2

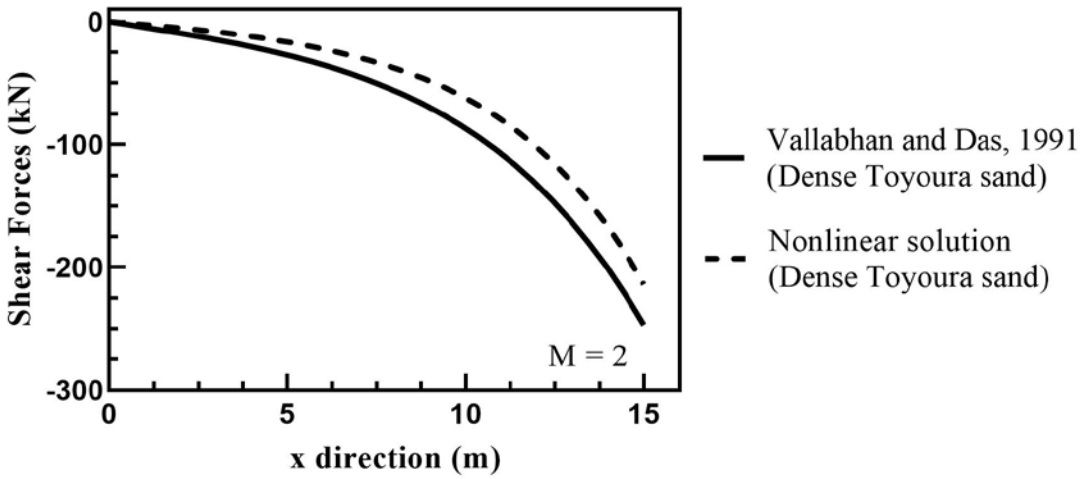

Figure 4.13 Dense Toyoura sand shear force results for M = 2

It has been observed that with increasing *M* values the difference between shear forces decreases as shown in Figure 4.10, Figure 4.11, Figure 4.12, and Figure 4.13. The magnitude of the shear force distributions found by the nonlinear solution is found lower than those of the linear solution for this specific geometry and material properties. Such behavior is also observed when a lower value of Es for soil is used in the linear analysis.

4.3. Example 2: Verification of Capturing Nonlinear Soil Behavior

In this example, it is verified that the proposed algorithm captures the nonlinear soil behavior by following the modulus reduction curves used for analysis. This will ensure that the reduced secant modulus values are used during the analysis at corresponding strain levels that emerged from the analysis. The geometry and material properties are kept the same as in the previous sections.

The main purpose of this comparison is to show whether the program is using G/G_{max} curves correctly. Shear strain values calculated by the program followed the values of the G/G_{max} curves entered into the program for loose Toyoura sand (Figure 4.2) and dense Toyoura sand (Figure 4.3) along the curve. The resulting shear strain and G_{sec} values showed that the program is processing the data correctly. The shear strain values calculated at the midpoint of the beam on the soil surface and the corresponding G/G_{max} values used in the analysis for the loose Toyoura sand and the dense Toyoura sand are given in Figure 4.14 and Figure 4.15, respectively.

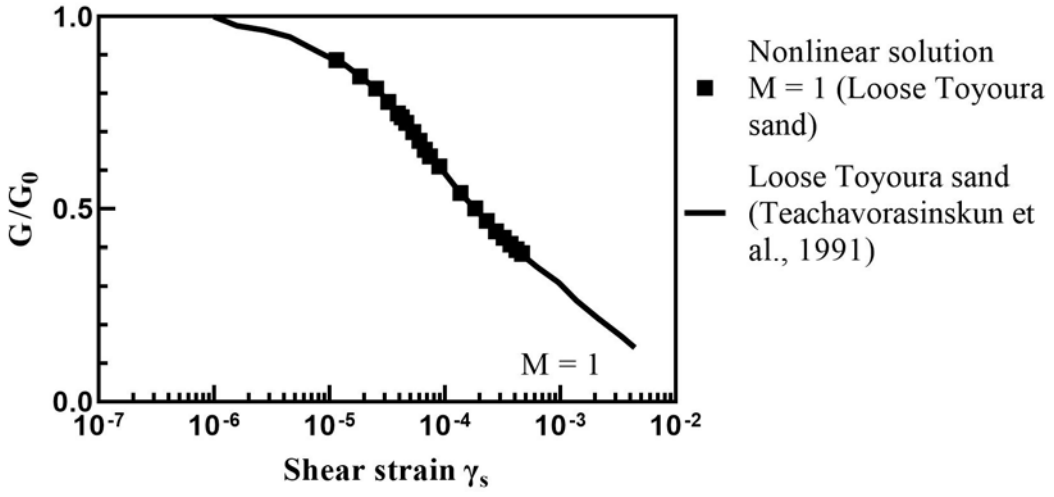

Figure 4.14 The nonlinear solution follows the shear modulus redution curve for loose Toyoura sand

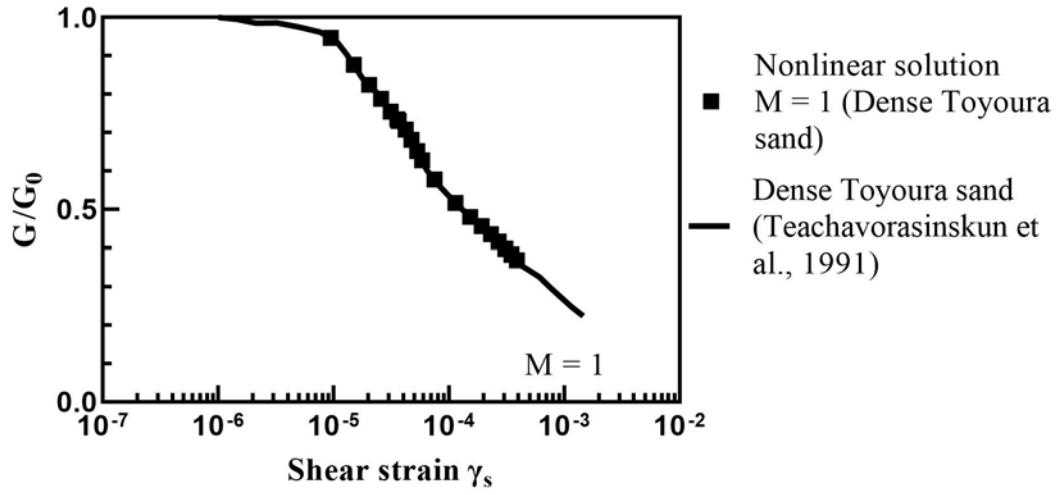

Figure 4.15 The nonlinear solution follows the shear modulus redution curve for dense Toyoura sand

As shown in Figure 4.14 and Figure 4.15, the G/G_{max} curves entered for the program, loose Toyoura sand and dense Toyoura sand matched the shear strain and G_{sec} values calculated in the program. This proves that the nonlinear G/G_{max} reduction curve is followed and employed properly in the analysis.

4.4. Example 3: Effect of Stiffness Increase and Soil Thickness

This example considers the effect of stiffness increase and the soil thickness on the response of the foundation by providing comparisons of deflection with non-dimensionalized parameters such as non-dimensionalized deflection (w) and thickness over the length of the beam, H/L, ratios. The soil stiffness increase is taken into account by the higher M values showing the linearly increasing stiffness of soil by depth. One should note that the higher M values represent the stiffer soil sections toward the bottom. H/L ratio is as important as M values since they both are the most significant non-dimensional parameters that affect the solution. Two different H/L ratios are considered in this example; H/L=0.5 and H/L=1, in which H is taken as H=15m and H=30m, respectively. The deflections compared for both M = 1 and M = 2 ratios are presented in Figure 4.16 and Figure 4.17. We provide the comparison of two soil types: linear soil by Vallabhan and Das (1988, 1991a) and nonlinear soil behavior (loose Toyoura sand).

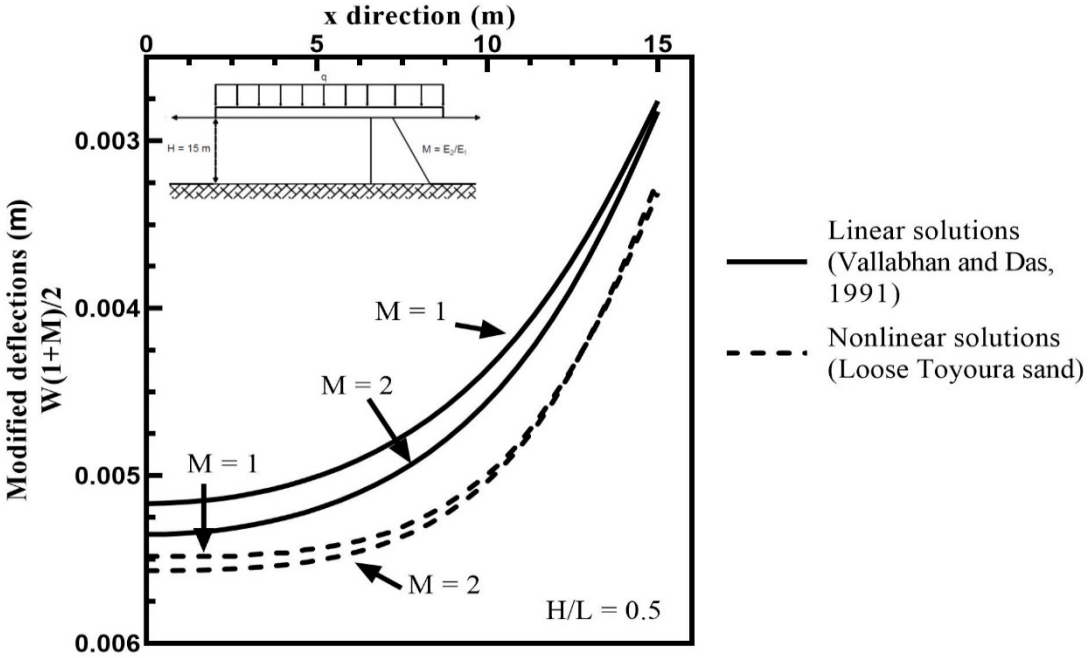

Figure 4.16 Deflection results for H/L = 0.5

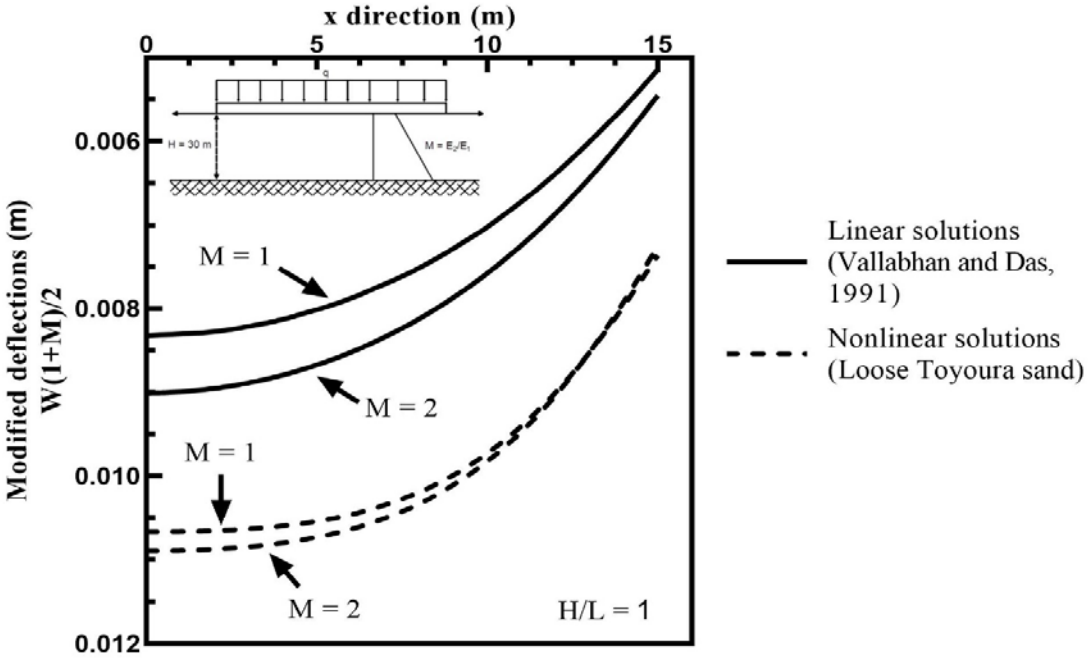

Figure 4.17 Deflection results for H/L = 1

With a higher H/L ratio the deflection values increase as given in Figures 4.16 and 4.17. The difference between linear and non-linear solutions is more noticeable in H/L=1 rather than it is in H/L=0.5. This indicates that as the depth of soil increases, nonlinearity is more effective.

4.5. Example 4: Comparison with the Finite Element Method

In this section, for the comparison of the finite element method (FEM), the geometry and material properties are kept the same as in section 4.1. A clear yield point could not be obtained from a hyperbolic stress-strain curve. Thus, this example uses a bilinear stress-strain curve to have a clear yield point which is required by the FE software. The yield point is taken as σ_y = 20 kPa and the corresponding strain is $\varepsilon_a = 10^{-3}$. E/E_{max} curve used in the analysis is shown in Figure 4.18. The FEM model is constructed by using quadratic elements to prevent hourglassing which occurs in the case of using linear elements with reduced integration. The developed method in this thesis is based on the work of Vallabhan and Das (1988, 1991a) which ignores the horizontal displacement; however, the FEM model considers the lateral movement in the domain, except on the right and left edges. To simulate the same example problem by the FE model, multiple sections are created underneath the beam and the horizontal displacements are constrained on these sections. However, the sections could only be applied to the element edges not the midpoint of the edges of quadratic elements. In addition, the soil domain that extends out of the beam is not constrained to prevent horizontal displacement which required creating many small sections. However, it would not be a practical and applicable approach. Therefore, only a limited number of sections were created under the beam.

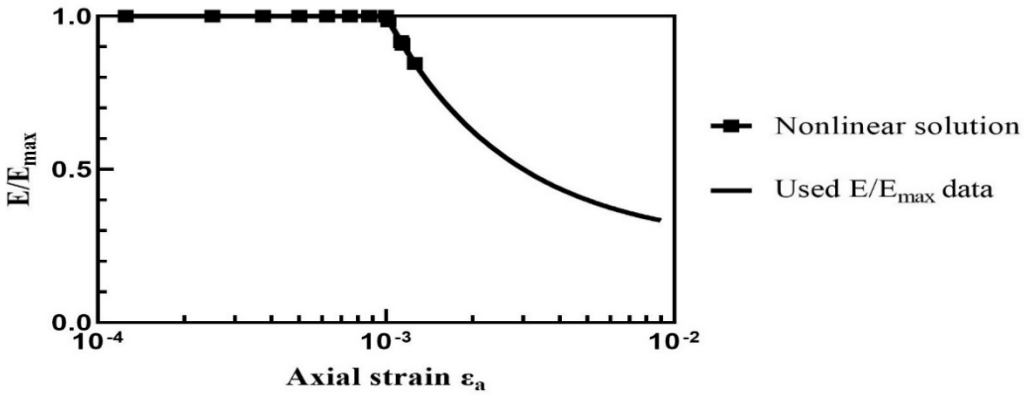

Figure 4.18 The modulus reduction curve used in the analysis

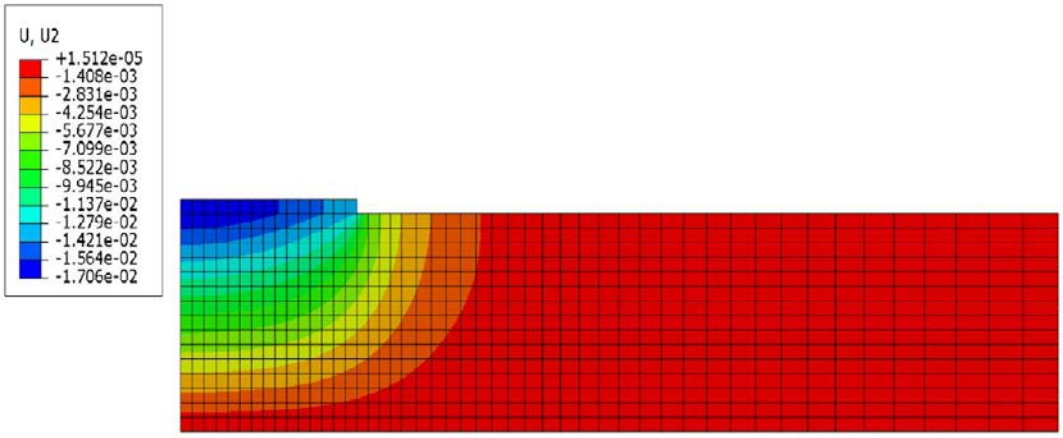

Figure 4.19 The finite element mesh used in the example and the results

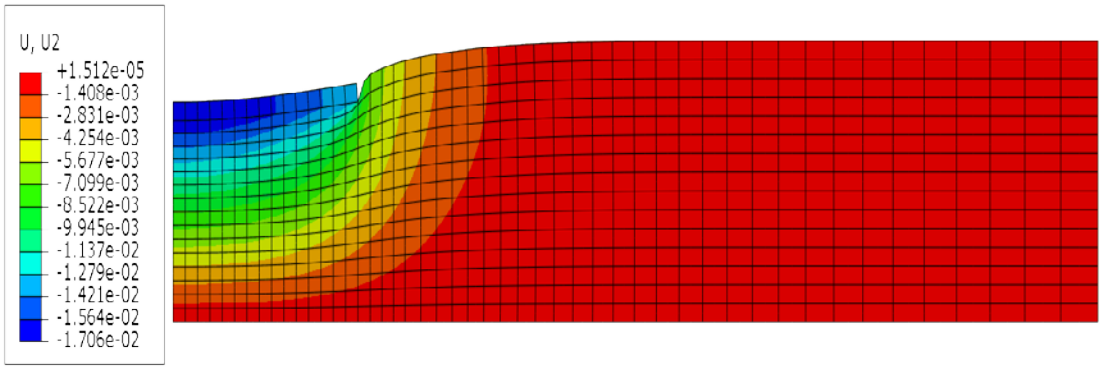

Figure 4.20 The deformed shape of the model

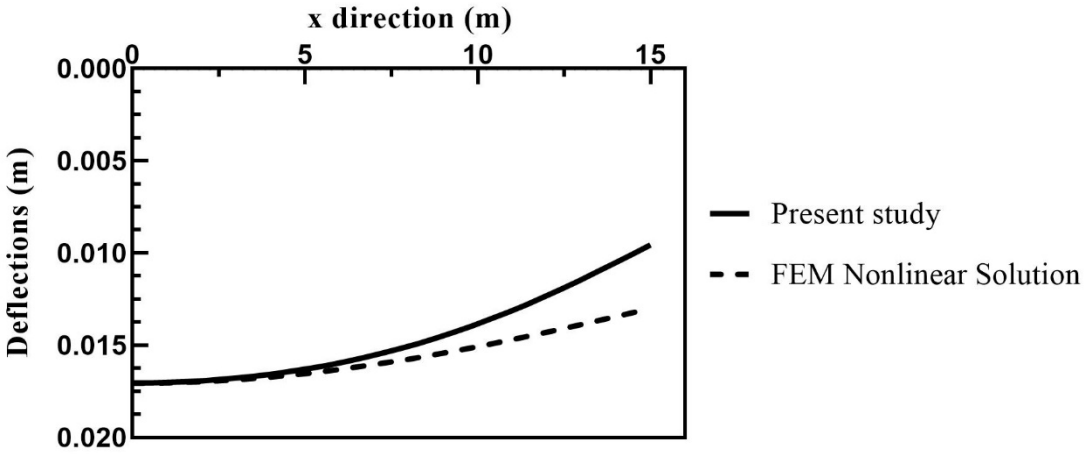

Figure 4.21 Comparison of the deflection results

The finite element mesh and deflection values in this example are shown in Figure 4.19. Also, the deformed shape of the model is given by using a scaling factor and it is presented in Figure 4.20. The maximum deflections obtained from the present study and the FE model matched well for this example as given in Figure 4.21. The difference toward the end of the beam might be the cause of the small horizontal displacements that occurred in the FE model, but such displacements could not be captured by the present study since the lateral displacement are assumed to be negligible and set to zero in the foundation. However, the FE analysis gave small but non-zero horizontal displacements.

CHAPTER 5

CONCLUSIONS

In this study, a new algorithm for the well-known modified Vlasov model to account for the soil nonlinearity within the context of modulus degradation curves was proposed. The new algorithm works efficiently and allows users to account for different shear modulus reduction curves easily. The results indicate that the contribution leads to different responses depending on the type of the shear modulus degradation curve used for soil stratum such as dense or loose soils. Numerical examples clearly exhibit the significant effect of the nonlinear soil behavior on the deflection, moment, and shear force and also present the effect of the initial stiffness increase by the depth and the strain-dependent modulus reduction. Also, there is a significant influence on the shape of the modulus degradation curves which will carry the characteristics of different types of soils. This new method is also compared with the FE model. The FE model gave a close match with the present study. Both methods present similar trends for the deflections of the foundation. In addition, this new method will provide users with the opportunity to avoid complicated constitutive model implementations and the laboratory experiments required by such models, but the simple load-deflection or shear force versus shear strain experiments can be employed to capture and take the nonlinearity into account for operational strain levels.

The present study can be developed to include the horizontal displacements of soil in the modified Vlasov model, which was neglected in the previous works and in the present study. The proposed approach to include nonlinear behavior of soils can also be applied to investigate the various foundation-structure interaction problems, for instance, the response of the plates on layered soils in three-dimensional problems; the response of the vertical machine foundations; laterally and axially loaded piles including damping ratio change. Such studies are envisioned as the future work of the present study.

REFERENCES

Allotey N., El Naggar, M.H. 2008. “Generalized dynamic Winkler model for nonlinear soil–structure interaction analysis”. Canadian Geotechnical Journal. 45(4): 560-573. https://doi.org/10.1139/T07-106

Aşık, M. Z. 1999. “Dynamic Response Analysis of the Machine Foundations on a Nonhomogeneous Soil Layer”. Journal of Computers and Geotechnics, 24, p.141-153.

Badoni, D., Makris, N. 1996. “Nonlinear response of single piles under lateral inertial and seismic loads”, Soil Dynamics and Earthquake Engineering, 15: 29–43. doi:10.1016/0267-7261(95) 00027-5.

Bhartiya, P., Chakraborty, T., Basu, D. 2020. “Nonlinear subgrade modulus of sandy soils for analysis of piled raft foundations”, Computers and Geotechnics, Volume 118, https://doi.org/10.1016/j.compgeo.2019.103350.

Boulanger, R.W., Curras, J.C., Kutter, B.L., Wilson, D.W., Abghari, A. 1999. “Seismic soil–pile–structure interaction experiments and analysis”, Journal of Geotechnical and Geoenvironmental Engineering, ASCE, 125: 750–759. doi:10.1061/ (ASCE)1090-0241(1999)125:9(750)

Chandra, S., Madhav, M.R., Iyengar, N.G.R. 1987. “A new model for nonlinear subgrades, Mathematical Modelling”, Volume 8, Pages 513-518, ISSN 0270-0255, https://doi.org/10.1016/0270-0255(87)90635-X.

Chen, W., C. Lü, and Z. Bian. 2004. “A mixed method for bending and free vibration of beams resting on a Pasternak elastic foundation.” Appl. Math. Modell. 28 (10): 877–890. https://doi.org/10.1016/j.apm.2004.04.001.

Daloglu, A., Vallabhan, C.V.G. 2000. “Values of k for Slab on Winkler Foundation”, Journal of Geotechnical and Geoenvironmental Engineering, 126. 10.1061/(ASCE)1090-0241(2000)126:5(463).

Das, B. M. 2010. “Geotechnical Engineering Handbook”. J. Ross Publishing, 1 edition.

Dutta, S., Roy, R. 2002. “A critical review on idealization and modeling for interaction among soil–foundation–structure system”, Computers & Structures,80,1579-1594. 10.1016/S0045-7949(02)00115-3.

El Naggar, M.H., Bentley, K.J. 2000. “Dynamic analysis for laterally loaded piles and dynamic p–y curves”, Canadian Geotechnical Journal, 37: 1166–1183. doi:10.1139/cgj-37-6-1166

Fahey, M. and Carter, J. 1993. “A finite element study of the pressuremeter using a nonlinear elastic plastic model”. Canadian Geotechnical Journal 30 (2), 348-362.

Filonenko-Borodich, M.M. 1945. “A Very Simple Model of an Elastic Foundation Capable of Spreading the Load”. Sb Tr. Mosk. Elektro. Inst. Inzh. Trans., No. 53, Transzheldorizdat.

Filonenko-Borodich, M.M. 1940. “Some Approximate Theories of the Elastic Foundation”. Uch. Zap. Mosk. Gos, Univ. Mekh. No. 46, 3-18.

Gerolymos, N., Gazetas, G. 2005. “Phenomenological model applied to inelastic response of soil–pile interaction systems”, Soils and Foundations, 45: 119–132.

Hardin, B.O., Drnevich, V.P. 1972b. “Shear modulus and damping in soils: design equations and curves”. Journal of the Soil Mechanics & Foundations Div. (ASCE) 98 (7), 667-692.

Hardin, B.O., Drnevich, V.P. 1972a. “Shear modulus and damping in soils: measurement and parameter effects”. Journal of the Soil Mechanics & Foundations Div. (ASCE) 98 (6), 603-624.

Isbuga, V. 2020. “Modeling of pile-soil-pile interaction in laterally loaded pile groups embedded in linear elastic soil layers”. Arabian Journal of Geosciences. 13. 10.1007/s12517-020-5229-8.

Ishibashi, I., Zhang, X. 1993. "Unified dynamic shear moduli and damping ratios of sand and clay," Soils and Foundations, Vol. 33, No. 1, pp. 182-191

Kagawa, T., Kraft, L.M. 1980. “Lateral load–deflection relationships of piles subjected to dynamic loading”. Soils and Foundations, 20: 19–36.

Kerr, A. D. 1964. “Elastic and Viscoelastic Foundation Models”. Journal of Applied Mechanics 31, 491-498

Kerr, A. D. 1965. “A Study of a New Foundation Model”. Acta Mechanica 1, 135–147. https://doi.org/10.1007/BF01174308

Kokoshu, T. 1980. "Cyclic triaxial test of dynamic soil properties for wide strain range," Soils and Foundations, Vol. 20, No. 2, pp. 45-60

Kramer, S. L. 1996. “Geotechnical Earthquake Engineering”. Prentice Hall, 1 edition.

Lo Presti, D., Pallara, O., Puci, I. 1995. "A Modified Commercial Triaxial Testing System for Small Strain Measurements: Preliminary Results on Pisa Clay," Geotechnical Testing Journal 18, no. 1: 15-31. https://doi.org/10.1520/GTJ10118J

Lo Presti, D.C.F., Pallara, O., Lancellotta, R., Armandi, M., Maniscalco, R. 1993. “Monotonic and cyclic loading behavior of two sands at small strains”, ASTM Geotechnical Testing Journal 16 (4), 409-424.

Mayne, P., Schneider, J. 2001. “Evaluating axial drilled shaft response by seismic cone”, Foundations and Ground Improvement. Pg: 655-669, GSP 113, ASCE.

Niazi, F., Mayne, P. 2014. “Axial pile response of bi-directional O-cell loading from modified analytical elastic solution and downhole shear wave velocity”. Canadian Geotechnical Journal. 51. 10.1139/cgj-2013-0220.

Nogami T., Lam, Y.C. 1987. “Two-parameter layer model for analysis of slab on elastic foundation.” J of Engng Mech, ASCE ;113(9):1279-1291.

Pasternak PL. 1954. “On a new method of analysis of an elastic foundation by means of two foundation constants”. Gosudarstvennogo Izatestvo Literaturi po Stroitelstvu i Architekutre, Moskow.

Reddy, J. N. 1984. “Energy and variational methods in applied mechanics”. John Wiley and Sons, New York, N.Y.

Schnabel, P.B., Lysmer, J., Seed, H.B. 1972. "SHAKE: A computer program for earthquake response analysis of horizontally layered sites," Report No. EERC 72-12, Earthquake Engineering Research Center, University of California, Berkeley, California.

Seed, H.B., Wong, R.T., Idriss, I.M., Tokimatsu, K. 1986. “Moduli and damping factors for dynamic analyses of cohesionless soils", Journal of Geotechnical Engineering, ASCE, Vol. 112, No. 11, pp. 1016-1032.

Seed, H.B.,Whitman, R.V.,and Lysmer, J. (1977). “Soil–structure interaction effects in the design of nuclear power plants”. In:Hall,W.J. (Ed.), Structural and Geotechnical Mechanics (Chapter13), a Volume Honoring Nathan M. Newmark. Prentice-Hall. Upper Saddle River, New Jersey.

Sun, K. 1994. “Laterally Loaded Piles in Elastic Media”. Journal of Geotechnical Engineering. 120. 10.1061/(ASCE)0733-9410(1994)120:8(1324).

Tatsuoka, F., Shibuya, S. 1992. “Deformation characteristics of soils and rocks from field and laboratory tests”. Report of the Institute of Industrial Science, Vol. 37, No. 1, Serial No. 235, The University of Tokyo, 136 p.

Teachavorasinskun, S., Shibuya, S., and Tatsuoka, F. 1991. “Stiffness of sands in monotonic and cyclic torsional simple shear”. Proceedings of the Geotechnical Engineering Congress, Geotechnical Engineering Division, American Society of Civil Engineering, Bolder, Colo., pp. 863-878.

Vallabhan, C.V.G., Das, Y.C. 1991a. “A refined model for beams on elastic foundations.” Int. J. Solids. Structures. ASCE;27(5):629-637.

Vallabhan, C.V.G., Das, Y.C. 1991b. “Modified Vlasov model for beams on elastic foundations.” J. Geotech. Engng. ASCE;117(6):956-66.

Vallabhan, C.V.G., Das, Y.C. A. 1988. “Parametric study of beams on elastic foundations.” J. Engng. Mech. ASCE ;114(2):2072-82.

Vlasov, V. Z., Leont'ev, N. N. 1966. "Beams, plates, and shells on elastic foundations,"Translated from Russian, Israel Program for Scientific Translations, Jerusalem.

Wang, C., Y. Xiang, and Q. Wang. 2001. “Axisymmetric buckling of Reddy circular plates on Pasternak foundation.” J. Eng. Mech. 127 (3): 254–259. https://doi.org/10.1061/(ASCE)0733-9399(2001) 127:3(254).

Winkler, E.1867. “Die Lehre Von Der Elastizitat Und Festigkeit.”, Prag Dominicus, Pages 182-184.

Younesian, D., Hosseinkhani, A., Askari, H., Esmailzadeh, E. 2019. “Elastic and viscoelastic foundations: a review on linear and nonlinear vibration modeling and applications”. Nonlinear Dyn 97, 853–895. https://doi.org/10.1007/s11071-019-04977-9

Zadeh, K.A. 2020. “Investigation of effects of soil-sturucture interaction on the seismic response of RC bridges using a performance-based design approach”. PhD Thesis, The University of British Columbia